hep-ph/0211467, November 2002

Collider Probes of the MSSM Higgs Sector with Explicit CP Violation

M. Carena[a], J. Ellis[b], S. Mrenna[a,f], A. Pilaftsis[a,c] and C.E.M. Wagner[d,e]

[a] *Fermilab, P.O. Box 500, Batavia IL 60510, U.S.A.*

[b] *Theory Division, CERN, CH-1211 Geneva 23, Switzerland*

[c] *Department of Physics and Astronomy, University of Manchester, Manchester M13 9PL, United Kingdom*

[d] *High Energy Physics Division, Argonne National Lab., Argonne IL 60439, U.S.A.*

[e] *Enrico Fermi Institute, University of Chicago, 5640 Ellis Ave., Chicago IL 60637, U.S.A.*

[f] *Michigan Center for Theoretical Physics, Randall Lab., University of Michigan, Ann Arbor, MI 48109, U.S.A.*

ABSTRACT

We investigate the hadron collider phenomenology of the Minimal Supersymmetric Standard Model (MSSM) with explicit CP violation for Higgs bosons that can be observed in Standard Model search channels: $W/ZH_i(\to b\bar{b})$ at the Tevatron, and $gg \to H_i(\to \gamma\gamma)$, $t\bar{t}H_i(\to b\bar{b})$ and $WW \to H_i(\to \tau^+\tau^-)$ at the LHC. Our numerical analysis is based on a benchmark scenario proposed earlier called CPX, which has been designed to showcase the effects of CP violation in the MSSM, and on several variant benchmarks. In most of the CPX parameter space, these hadron colliders will find one of the neutral MSSM Higgs bosons. However, there are small regions of parameter space in which none of the neutral Higgs bosons can be detected in the standard channels at the Tevatron and the LHC. This occurs because the neutral Higgs boson with the largest coupling to W and Z bosons decays predominantly into either two lighter Higgs bosons or a Higgs boson and a gauge boson, whilst the lighter Higgs boson has only small couplings to the W and Z bosons and the top quark. For other choices of CP-violating parameters, all three neutral Higgs bosons can have significant couplings to W and Z bosons, producing overlapping signatures: these may or may not be distinguishable from backgrounds. The existence of these regions of parameters provides a strong motivation for a detailed experimental simulation of these channels.

1 Introduction

Detailed studies of the mechanism of electroweak symmetry breaking top the agendas of operating particle accelerators, as well as those under construction or being proposed for the near future. One paradigm for many of these studies is provided by the minimal supersymmetric extension of the Standard Model (MSSM) [1]. There is increasing interest in the possibility that the MSSM includes explicit CP violation, which may provide opportunities to probe CP violating parameters through the Higgs sector [2–13].

Assuming universality of the soft supersymmetry (SUSY)-breaking gaugino masses $m_{1/2}$, scalar masses m_0 and trilinear parameters A_0 at the Grand Unification Theory (GUT) input scale, the MSSM then provides only two new sources of CP violation in addition to the Kobayashi–Maskawa phase of the Standard Model (SM). In a suitable convention, these may be represented as the phases of complex parameters $m_{1/2}$ and A_0. The values of these phases are constrained by the upper limits on the electric dipole moments (EDMs) of the electron, neutron [14, 15] and mercury atom [16] and other measurements. The ongoing probes of CP violation at B factories can also test the consistency of the above minimal CP-violating supersymmetric scenario [17, 18].

In the MSSM with explicit CP violation, the effect of CP violation on the Higgs sector enters beyond the Born approximation [2,3]. The effects [3–7] induced by $\arg(A_0)$ and $\arg(m_{1/2})$ on the MSSM Higgs-boson masses have been studied in some detail [6,9]. Several interesting phenomenological implications for the Higgs bosons emerge in this minimal CP-violating framework of the MSSM. The three neutral Higgs bosons (h and H, which have scalar couplings to fermions at the tree level, and A with pseudoscalar tree-level couplings to fermions), all mix together in the presence of CP violation. The resulting three physical mass eigenstates have mixed CP parities. We denote these by $H_{1,2,3}$ in order of increasing masses, i.e., $M_{H_1} \leq M_{H_2} \leq M_{H_3}$. As a consequence of CP violation, all the three neutral Higgs bosons can now have tree–level couplings to pairs of $W^\pm$ and Z bosons. The Higgs couplings to the gauge bosons obey the sum rules

$$\sum_{i=1}^{3} g^2_{H_i W^+ W^-} \;=\; g^2_{HW^+W^-}\,, \qquad \sum_{i=1}^{3} g^2_{H_i ZZ} \;=\; g^2_{HZZ}\,, \tag{1.1}$$

where $g_{HW^+W^-}$ and g_{HZZ} are the Standard Model couplings. Additionally, there is an important complementarity relation between the H_iZZ and H_iH_jZ couplings:

$$g_{H_iH_jZ} \;=\; \varepsilon_{ijk}\, g_{H_kZZ}\,, \tag{1.2}$$

where ε_{ijk} is the fully anti-symmetric Levi–Civita tensor. We have shown that the phenomenological consequences of (1.1) and (1.2) can be dramatic [6]. In particular, (1.1)

implies that the H_1ZZ coupling can be significantly suppressed, thus raising the possibility that a relatively light H_1 boson, with a mass even as low as 60 GeV, might have escaped detection at LEP 2. On the other hand, (1.2) leaves open the possibility of H_1H_2 production at LEP 2, as discussed below. However, this brief discussion highlights the fact that a large part of the parameter space related to the Higgs sector must be re-explored in the presence of CP violation.

In this paper, we investigate systematically the physics potential of the Standard Model Higgs boson searches at the Tevatron collider and the LHC for observing neutral Higgs bosons in the MSSM with explicit CP violation. We focus on Standard Model search channels, since the existence of a light Higgs boson with a significant coupling to W and Z bosons is a prediction of weak–scale supersymmetry. The present work goes beyond previous work on this subject [10] by incorporating the most important radiative corrections to the Higgs sector and performing a numerical analysis based on the most realistic simulations of Standard Model Higgs boson searches at the Tevatron and LHC. Our phenomenological study is performed mainly within the context of the CPX scenario [8], which was chosen to showcase the possible effect of CP violation in the Higgs sector of the MSSM. Given the limits from the LEP collider and existing simulations of the capabilities of the Tevatron and the LHC, we show that there are small regions of parameters in which all three neutral Higgs bosons escape detection. In these regions of parameters, the heavier Higgs bosons with the dominant coupling to the W and Z boson decay into Higgs boson with a tiny coupling to the W and Z boson, or into a lighter Higgs boson and a gauge boson. Outside these small regions of parameters, our analysis indicates, even in the presence of CP violation, the discovery of at least one neutral MSSM Higgs boson in a set of complementary detection channels. This provides a strong motivation to extend the experimental simulations to Higgs boson decay channels containing lighter Higgs boson states. For other choices of CP-violating parameters, we find that all three neutral Higgs bosons can have significant couplings to W and Z bosons, while being closely spaced in mass. This situation also requires careful investigation, since some signals may be affecting the background estimates for other signals.

Our numerical analysis is performed using the code `CPHDECAY` [19], which is based on an extension of the code `HDECAY` [20] to calculate the Higgs boson decay properties, and of the code `cph` [6,21] to calculate the physical Higgs spectrum and mixing angles. The latter code includes the dominant one- and two-loop CP-violating contributions induced by the supersymmetric particles. At one loop, these contributions depend mostly on the phase of the trilinear mass parameters of the third-generation quarks, $A_{t,b}$, relative to that of the supersymmetric mass parameter μ^*. At the two-loop level, a significant dependence on the

relative phase between μ^* and the gluino mass parameter $m_{\tilde{g}}$ also appears. Electroweak corrections are incorporated at the leading-logarithmic level. In a phase convention where the μ parameter is positive, the input parameters for the code are the top-quark mass m_t, the μ parameter, the soft supersymmetry-breaking masses $\widetilde{M}_Q^2$, $\widetilde{M}_{t,b}^2$ of the third-generation squarks, the third-generation soft trilinear couplings $A_{t,b}$ together with their respective phases, the gaugino masses and the phase of the gluino mass parameter $m_{\tilde{g}}$. Apart from its present application to hadron colliders, `CPHDECAY` may also serve as a useful tool for analogous studies at future linear e^+e^- colliders [11] or a muon collider [12], or for generic Higgs boson studies [13].

Section 2 contains a complete discussion of the effective couplings of the neutral and charged Higgs bosons to quarks and of the Higgs self-couplings; full expressions are given in Appendix A. The one-loop corrected Higgs couplings are essential, as they determine the branching ratios of the Higgs bosons in the presence of CP violation. Section 3 contains a discussion of the LEP results in the search for neutral Higgs bosons in the MSSM with explicit CP violation. Section 4 contains a numerical analysis of the different collider detection channels, showing graphically their complementary properties for the detection of Standard Model–like Higgs bosons in the MSSM with explicit CP violation. We restrict ourselves to the existing experimental simulations, identifying regions of parameters at small values of $\tan\beta$ and of the charged Higgs boson mass, for which none of the neutral Higgs bosons can be detected at the Tevatron or the LHC via the standard search channels. Our conclusions are presented in Section 5. Appendix A contains detailed formulae for couplings and Appendix B summarizes the information from detector simulations on which we base our analysis [22, 24, 23, 26].

2 Effective Higgs-Boson Couplings

In order to study the collider phenomenology of the Higgs bosons in the MSSM with explicit CP violation, we must first calculate the couplings of the Higgs bosons to Standard Model and MSSM particles. In this section, we present explicitly those couplings which are the most important inputs to our numerical calculations. In particular, we review the effective couplings of the neutral Higgs bosons to quarks, and we present the effective Higgs self-couplings. We also give the corresponding effective couplings of the charged Higgs boson to the up and down quarks, even though they are not needed for the present analysis.

2.1 Effective Higgs-boson couplings to quarks

Following our previous conventions throughout this paper [6], we define the physical scalar components of the Higgs superfields $\widehat{H}_1$ and $\widehat{H}_2$ as $\widetilde{\Phi}_1 = i\tau_2\,\Phi_1^* = (\phi_1^{0*},\ -\phi_1^-)$ and $\Phi_2 = (\phi_2^+,\ \phi_2^0)$, respectively, where τ_2 is the usual Pauli matrix. The weak Higgs eigenstates are related to their mass eigenstates H^+ and $H_{1,2,3}$ through the orthogonal transformations:

$$\begin{aligned}
\phi_1^+ &= \cos\beta\, G^+ \,-\, \sin\beta\, H^+\,, \qquad \phi_2^+ \;=\; \sin\beta\, G^+ \,+\, \cos\beta\, H^+\,, && (2.1)\\
\phi_1^0 &= \tfrac{1}{\sqrt{2}}\Big[\, v_1 \,+\, O_{1i}\, H_i \,+\, i\Big(\cos\beta\, G^0 \,-\, \sin\beta\, O_{3i}\, H_i\Big)\Big]\,, && \\
\phi_2^0 &= \tfrac{1}{\sqrt{2}}\Big[\, v_2 \,+\, O_{2i}\, H_i \,+\, i\Big(\sin\beta\, G^0 \,+\, \cos\beta\, O_{3i}\, H_i\Big)\Big]\,, && (2.2)
\end{aligned}$$

where G^+ and G^0 are the would-be Goldstone bosons associated with the W^+ and Z bosons, respectively, and O is a 3-by-3 orthogonal matrix that describes the mixing of the neutral Higgs states in the presence of CP violation [3].

Our starting point is the effective Lagrangian for the neutral Higgs-boson couplings to the u- and d-type quarks. We neglect quark-mixing effects, as their direct relevance to Higgs searches is not important.[1] Moreover, we assume that there is negligible mixing between the different generations of squarks, and we include weak-interaction effects only at the leading-logarithmic level.

Under these assumptions, the effective Lagrangian reads:

$$\begin{aligned}
-\,\mathcal{L}^0_{\rm eff} \;=\; & \Big[\,(h_d \,+\, \delta h_d)\,\phi_1^{0*} \,+\, \Delta h_d\,\phi_2^{0*}\,\Big]\,\bar{d}_R\, d_L \\
& + \Big[\,\Delta h_u\,\phi_1^0 \,+\, (h_u \,+\, \delta h_u)\,\phi_2^0\,\Big]\,\bar{u}_R\, u_L \;+\; \text{h.c.}, \qquad (2.3)
\end{aligned}$$

where $\delta h_{d,u}/h_{d,u}$ and $\Delta h_{d,u}/h_{d,u}$ are threshold radiative effects given by

$$\begin{aligned}
\frac{\delta h_d}{h_d} &= -\frac{2\alpha_s}{3\pi}\, m_{\tilde{g}}^*\, A_d\, I(m^2_{\tilde{d}_1}, m^2_{\tilde{d}_2}, |m_{\tilde{g}}|^2) \;-\; \frac{|h_u|^2}{16\pi^2}\,|\mu|^2\, I(m^2_{\tilde{u}_1}, m^2_{\tilde{u}_2}, |\mu|^2)\,, && (2.4)\\
\frac{\Delta h_d}{h_d} &= \frac{2\alpha_s}{3\pi}\, m_{\tilde{g}}^*\, \mu^* I(m^2_{\tilde{d}_1}, m^2_{\tilde{d}_2}, |m_{\tilde{g}}|^2) \;+\; \frac{|h_u|^2}{16\pi^2}\, A_u^*\mu^*\, I(m^2_{\tilde{u}_1}, m^2_{\tilde{u}_2}, |\mu|^2)\,, && (2.5)\\
\frac{\Delta h_u}{h_u} &= \frac{2\alpha_s}{3\pi}\, m_{\tilde{g}}^*\mu^*\, I(m^2_{\tilde{u}_1}, m^2_{\tilde{u}_2}, |m_{\tilde{g}}|^2) \;+\; \frac{|h_d|^2}{16\pi^2}\, A_d^*\mu^*\, I(m^2_{\tilde{d}_1}, m^2_{\tilde{d}_2}, |\mu|^2)\,, && (2.6)\\
\frac{\delta h_u}{h_u} &= -\frac{2\alpha_s}{3\pi}\, m_{\tilde{g}}^*\, A_u\, I(m^2_{\tilde{u}_1}, m^2_{\tilde{u}_2}, |m_{\tilde{g}}|^2) \;-\; \frac{|h_d|^2}{16\pi^2}\,|\mu|^2\, I(m^2_{\tilde{d}_1}, m^2_{\tilde{d}_2}, |\mu|^2)\,. && (2.7)
\end{aligned}$$

We would like to emphasize that no other work includes the Δh_b corrections, and that these have important phenomenological implications, as we discuss below.

[1] For a recent discussion of CP-violating Higgs-mediated flavor-changing neutral-current effects on low-energy observables, see Ref. [18].

In (2.4)–(2.7), $\alpha_s = g_s^2/(4\pi)$ is the SU(3)$_c$ fine-structure constant, $I(a,b,c)$ is the function

$$I(a,b,c) \equiv \frac{ab\ln(a/b) + bc\ln(b/c) + ac\ln(c/a)}{(a-b)(b-c)(a-c)} , \tag{2.8}$$

and $m_{\tilde{q}_1,\tilde{q}_2}$ (with $q = u,d$) are the squark masses, with

$$m^2_{\tilde{q}_1\,(\tilde{q}_2)} = \frac{1}{2}\Big\{ \widetilde{M}_Q^2 + \widetilde{M}_q^2 + 2\,m_q^2 + T_z^q \cos 2\beta M_Z^2 \tag{2.9}$$
$$+(-)\sqrt{\Big[\,\widetilde{M}_Q^2 - \widetilde{M}_q^2 + \cos 2\beta M_Z^2\,(T_z^q - 2Q_q \sin^2\theta_w)\,\Big]^2 + 4\,m_q^2\,|A_q - R_q\mu^*|^2}\;\Big\},$$

and $Q_u\,(Q_d) = 2/3\,(-1/3)$, $T_z^u = -T_z^d = 1/2$, $R_u\,(R_d) = \cot\beta\ (\tan\beta)$, and $\sin^2\theta_w = 1 - M_W^2/M_Z^2$. In (2.3), the complex Yukawa couplings h_d and h_u are defined in a way such that the d- and u-quark masses are real and positive after the inclusion of radiative corrections, namely

$$h_d = \frac{m_d}{v\cos\beta}\,\frac{1}{1 + (\delta h_d/h_d) + (\Delta h_d/h_d)\tan\beta} , \tag{2.10}$$

$$h_u = \frac{m_u}{v\sin\beta}\,\frac{1}{1 + (\delta h_u/h_u) + (\Delta h_u/h_u)\cot\beta} . \tag{2.11}$$

Substituting (2.2) and (2.10) into (2.3), the effective Lagrangian for the $H_i\bar{q}q$ couplings can be written in the general form:

$$\mathcal{L}_{H_i\bar{q}q} = -\sum_{q=u,d}\frac{g_w m_q}{2M_W}\sum_{i=1}^{3} H_i\,\bar{q}\left(g^S_{H_i\bar{q}q} + i g^P_{H_i\bar{q}q}\gamma_5\right) q , \tag{2.12}$$

with [6, 15]

$$g^S_{H_i\bar{d}d} = \mathrm{Re}\left(\frac{1}{1 + \kappa_d\,\tan\beta}\right)\frac{O_{1i}}{\cos\beta} + \mathrm{Re}\left(\frac{\kappa_d}{1 + \kappa_d\,\tan\beta}\right)\frac{O_{2i}}{\cos\beta}$$
$$+\,\mathrm{Im}\left[\frac{\kappa_d\,(\tan^2\beta + 1)}{1 + \kappa_d\,\tan\beta}\right] O_{3i} , \tag{2.13}$$

$$g^P_{H_i\bar{d}d} = -\,\mathrm{Re}\left(\frac{\tan\beta - \kappa_d}{1 + \kappa_d\tan\beta}\right) O_{3i} + \mathrm{Im}\left(\frac{\kappa_d\,\tan\beta}{1 + \kappa_d\,\tan\beta}\right)\frac{O_{1i}}{\cos\beta}$$
$$-\,\mathrm{Im}\left(\frac{\kappa_d}{1 + \kappa_d\,\tan\beta}\right)\frac{O_{2i}}{\cos\beta} , \tag{2.14}$$

$$g^S_{H_i\bar{u}u} = \mathrm{Re}\left(\frac{1}{1 + \kappa_u\,\cot\beta}\right)\frac{O_{2i}}{\sin\beta} + \mathrm{Re}\left(\frac{\kappa_u}{1 + \kappa_u\,\cot\beta}\right)\frac{O_{1i}}{\sin\beta}$$
$$+\,\mathrm{Im}\left[\frac{\kappa_u\,(\cot^2\beta + 1)}{1 + \kappa_u\,\cot\beta}\right] O_{3i} , \tag{2.15}$$

$$g^P_{H_i\bar{u}u} = -\,\mathrm{Re}\left(\frac{\cot\beta - \kappa_u}{1 + \kappa_u\,\cot\beta}\right) O_{3i} + \mathrm{Im}\left(\frac{\kappa_u\,\cot\beta}{1 + \kappa_u\,\cot\beta}\right)\frac{O_{2i}}{\sin\beta}$$
$$-\,\mathrm{Im}\left(\frac{\kappa_u}{1 + \kappa_u\,\cot\beta}\right)\frac{O_{1i}}{\sin\beta} . \tag{2.16}$$

In the above, we have used the abbreviation: $\kappa_q = (\Delta h_q/h_q)/[1 + (\delta h_q/h_q)]$, for $q = u, d$, and the fact that u- and d-quark masses are real and positive, so that $\mathrm{Im}\, m_d \propto \mathrm{Im}\,[h_d + (\delta h_d) + (\Delta h_d)\tan\beta] = 0$ and $\mathrm{Im}\, m_u \propto \mathrm{Im}\,[h_u + (\delta h_u) + (\Delta h_u)\cot\beta] = 0$.

Though our phenomenological analysis is restricted to the neutral Higgs-boson sector, we consider for completeness the charged–Higgs–quark sector. The effective Lagrangian describing the interactions of the charged–Higgs fields $\phi^+_{1,2}$ with u and d quarks is given by

$$\begin{aligned} -\mathcal{L}^{\pm}_{\rm eff} &= \Big[\,(h_d \,+\, \bar\delta h_d)\,\phi_1^- \,+\, \bar\Delta h_d\,\phi_2^-\,\Big]\,\bar d_R\, u_L \\ &\quad - \Big[\,\bar\Delta h_u\,\phi_1^+ \,+\, (h_u \,+\, \bar\delta h_u)\,\phi_2^+\,\Big]\,\bar u_R\, d_L \;+\; \text{h.c.} \end{aligned} \tag{2.17}$$

The quantities $\bar\delta h_{u,d}$ and $\bar\Delta h_{u,d}$ contain the respective threshold radiative effects that affect the charged–Higgs couplings to quarks. Though they are related to the δh_q and Δh_q given above for the neutral Higgs sector, they differ by $\mathrm{SU}(2)_L$-breaking terms.

To facilitate our presentation of the analytic forms of $\bar\delta h_q$ and $\bar\Delta h_q$, we first set up our conventions for the squark-mixing parameters and define some auxiliary functions. Thus, the left- and right-handed squark fields $\tilde q_L$ and $\tilde q_R$ are related to the physical fields $\tilde q_{1,2}$ through the transformations:

$$\begin{aligned} \tilde q_L &= c_q\,\tilde q_1 \,+\, s_q\,\tilde q_2 \\ \tilde q_R &= -\,e^{i\delta_q}\,s_q\,\tilde q_1 \,+\, e^{i\delta_q}\,c_q\,\tilde q_2 \end{aligned} \tag{2.18}$$

where $\delta_q = \arg(A_q - R_q\mu^*)$ and $c_q = \cos\theta_{\tilde q}$ and $s_q = \sin\theta_{\tilde q}$ are squark-mixing angles. Analytic expressions for c_q and s_q may be found in Appendix A of [9]. We introduce the following short-hand form for the squark-loop integrals:

$$I(i,j,m) \;=\; I(m^2_{\tilde u_i}, m^2_{\tilde d_j}, |m|^2)\,, \tag{2.19}$$

where the indices i and j refer to the third-generation up- and down-squark mass eigenstates.

With the aid of (2.19), the following two auxiliary functions can be defined:

$$I_1(m) \;=\; c_u^2 s_d^2 I(1,1,m) \,+\, s_u^2 c_d^2 I(2,2,m) \,+\, c_u^2 c_d^2 I(1,2,m) \,+\, s_u^2 s_d^2 I(2,1,m)\,, \tag{2.20}$$

$$I_2(m) \;=\; s_u^2 c_d^2 I(1,1,m) \,+\, c_u^2 s_d^2 I(2,2,m) \,+\, s_u^2 s_d^2 I(1,2,m) \,+\, c_u^2 c_d^2 I(2,1,m)\,. \tag{2.21}$$

Again, in the limit of neglecting mixing of generations, the threshold radiative effects related to the charged Higgs sector can be expressed in terms of (2.20) and (2.21) as follows:

$$\frac{\bar\delta h_d}{h_d} \;=\; -\,\frac{2\alpha_s}{3\pi}\,m^*_{\tilde g} A_d\, I_1(m_{\tilde g}) \;-\; \frac{|h_u|^2}{16\pi^2}\,|\mu|^2\, I_2(\mu)\,, \tag{2.22}$$

$$\frac{\bar{\Delta} h_d}{h_d} \;=\; \frac{2\alpha_s}{3\pi}\, m^*_{\tilde{g}} \mu^*\, I_1(m_{\tilde{g}}) \;+\; \frac{|h_u|^2}{16\pi^2}\, \mu^* A^*_u\, I_2(\mu)\,, \tag{2.23}$$

$$\frac{\bar{\delta} h_u}{h_u} \;=\; -\frac{2\alpha_s}{3\pi}\, m^*_{\tilde{g}} A_u\, I_2(m_{\tilde{g}}) \;-\; \frac{|h_d|^2}{16\pi^2}\, |\mu|^2\, I_1(\mu)\,, \tag{2.24}$$

$$\frac{\bar{\Delta} h_u}{h_u} \;=\; \frac{2\alpha_s}{3\pi}\, m^*_{\tilde{g}} \mu^*\, I_2(m_{\tilde{g}}) \;+\; \frac{|h_d|^2}{16\pi^2}\, \mu^* A^*_b\, I_1(\mu)\,. \tag{2.25}$$

Then, the effective Lagrangian for the charged Higgs-boson couplings to u- and d-type quarks is given by

$$\mathcal{L}_{H^\pm ud} \;=\; \frac{g_w}{2M_W}\, H^+\, \bar{u} \Big(m_u\, g^L_{H^+\bar{u}d}\, P_- \;+\; m_d\, g^R_{H^+\bar{u}d}\, P_+ \Big)\, d \;+\; \text{h.c.}, \tag{2.26}$$

where $P_\mp = [1 \mp \gamma_5]/2$, and

$$g^L_{H^+\bar{u}d} \;=\; \frac{\cot\beta\,(1 \,+\, \rho_u) \;-\; \bar{\kappa}_u}{1 \,+\, \kappa_u\, \cot\beta}\,, \tag{2.27}$$

$$g^R_{H^+\bar{u}d} \;=\; \frac{\tan\beta\,(1 \,+\, \rho^*_d) \;-\; \bar{\kappa}^*_d}{1 \,+\, \kappa^*_d\, \tan\beta}\,. \tag{2.28}$$

The quantities $\kappa_{u,d}$ are given after (2.16), while $\bar{\kappa}_{u,d}$ and $\rho_{u,d}$ in (2.27) and (2.28) are defined as follows:

$$\bar{\kappa}_q \;=\; \frac{(\bar{\Delta} h_q/h_q)}{1 + (\delta h_q/h_q)}\,, \qquad \rho_q \;=\; \frac{(\bar{\delta} h_q/h_q) \;-\; (\delta h_q/h_q)}{1 + (\delta h_q/h_q)}\,, \tag{2.29}$$

with $q = u, d$, respectively.

It is apparent that the effective couplings of the neutral and charged Higgs bosons to quarks can be written in a form that depends entirely on the parameters $\kappa_{u,d}$, $\bar{\kappa}_{u,d}$ and $\rho_{u,d}$. It is technically interesting to note that all these quantities are renormalization-scale independent up to the one-loop order in our resummation approach. More explicitly, $\kappa_{u,d}$ and $\bar{\kappa}_{u,d}$ are proportional to the non-holomorphic radiative corrections $(\Delta h_{u,d}/h_{u,d})$ and $(\bar{\Delta} h_{u,d}/h_{u,d})$, respectively, which are manifestly scale-independent. The quantities $\rho_{u,d}$ are measures of $\text{SU}(2)_L$ breaking in the up- and down-Yukawa sectors. The parameters $\rho_{u,d}$ are also renormalization-scale independent, as a consequence of the $\text{SU}(2)_L$ gauge invariance of the original theory before spontaneous symmetry breaking. The scale independence of $\rho_{u,d}$ can be also understood by simply noticing that the ultra-violet infinities, e.g., of δh_d and $\bar{\delta} h_d$ are equal, as they emanate from the charged and neutral Higgs components of the same gauge-invariant operator, which is $\widehat{Q}\widehat{H}_1\widehat{D}$ in this case. The scale independence of these quantities has some analogies with that of Veltman's ρ parameter that characterizes the isospin breaking in the SM gauge sector through the difference between the WW and ZZ self-energies, that we do not develop further here.

Finally, we should bear in mind that the validity of the effective neutral and charged Higgs-boson couplings to quarks depend on two kinematic conditions: (i) the soft supersymmetry-breaking masses should be much larger than the electroweak scale and (ii) the external momenta of the quarks and Higgs bosons, e.g., $p_{q,H}$, have to be sufficiently smaller than the soft supersymmetry-breaking mass scale $M_{\rm SUSY}$, so that they can be neglected when expanding the vertex functions in powers of $p^2_{q,H}/M^2_{\rm SUSY}$.

2.2 Effective Higgs-boson self-couplings

To determine the effective Higgs self-couplings, one needs to know the analytic forms of both the proper vertex and self-energy graphs. So far, there is complete information only for the latter contributions in the MSSM with explicit CP violation [6,9], while the former effects have been computed in [3], in an expansion of the effective potential up to operators of dimension 4.

Here, we combine the above two pieces of information to obtain approximate analytic expressions for the trilinear and quadrilinear Higgs-boson self-couplings.[2] Our analytic expressions are not limited to the MSSM case, but can be applied equally well to the general Two-Higgs-Doublet Model (2HDM) with explicit CP violation.

To start with, we first write down the effective Lagrangian containing all operators of dimension 4:

$$\begin{aligned}\mathcal{L}^{\rm 4d}_{\rm eff} &= \lambda_1\,(\Phi_1^\dagger\Phi_1)^2 \,+\, \lambda_2\,(\Phi_2^\dagger\Phi_2)^2 \,+\, \lambda_3\,(\Phi_1^\dagger\Phi_1)\,(\Phi_2^\dagger\Phi_2) \,+\, \lambda_4\,(\Phi_1^\dagger\Phi_2)\,(\Phi_2^\dagger\Phi_1) \\ &\quad + \lambda_5\,(\Phi_1^\dagger\Phi_2)^2 \,+\, \lambda_5^*\,(\Phi_2^\dagger\Phi_1)^2 \,+\, \lambda_6\,(\Phi_1^\dagger\Phi_1)\,(\Phi_1^\dagger\Phi_2) \,+\, \lambda_6^*\,(\Phi_1^\dagger\Phi_1)\,(\Phi_2^\dagger\Phi_1) \\ &\quad + \lambda_7\,(\Phi_2^\dagger\Phi_2)\,(\Phi_1^\dagger\Phi_2) \,+\, \lambda_7^*\,(\Phi_2^\dagger\Phi_2)\,(\Phi_2^\dagger\Phi_1)\,, \end{aligned} \tag{2.30}$$

where $\Phi^T_{1,2} = (\phi^+_{1,2},\, \phi^0_{1,2})$ are the two Higgs doublets, with their individual charged and neutral components defined in (2.1) and (2.2). After (2.1) and (2.2) have been inserted into (2.30), the effective trilinear and quartic Higgs self-couplings may be cast into the form (in the unitary gauge):

$$\mathcal{L}^{\rm 3H}_{\rm eff} = v\left(\Gamma^{\rm 3H}_{ijk}\,H_iH_jH_k \,+\, \Gamma^{HH^+H^-}_i\,H_iH^+H^-\right), \tag{2.31}$$

$$\mathcal{L}^{\rm 4H}_{\rm eff} = \Gamma^{\rm 4H}_{ijkl}\,H_iH_jH_kH_l \,+\, \Gamma^{\rm 2HH^+H^-}_{ij}\,H_iH_jH^+H^- \,+\, \Gamma^{\rm 4H^+}\,(H^+H^-)^2\,, \tag{2.32}$$

where $v = \sqrt{v_1^2+v_2^2} \simeq 246$ GeV is the SM vacuum expectation value. The couplings $\Gamma^{\rm 3H}_{ijk}$ and $\Gamma^{\rm 4H^+}$ are given by

$$\Gamma^{\rm 3H}_{ijk} = \sum_{l\le m\le n=1,2,3} O_{li}\,O_{mj}\,O_{nk}\;g^{\rm 3H}_{lmn}\,, \qquad \Gamma^{HH^+H^-}_i = \sum_{l=1,2,3} O_{li}\;g^{HH^+H^-}_l\,, \tag{2.33}$$

[2] A similar procedure has been followed in Ref. [27].

$$\Gamma^{4H}_{ijkl} = \sum_{m\leq n\leq r\leq s=1,2,3} O_{mi}\, O_{nj}\, O_{rk}\, O_{sl}\; g^{4H}_{mnrs}\,, \qquad \Gamma^{2HH^+H^-}_{ij} = \sum_{l\leq m=1,2,3} O_{li}\, O_{mj}\; g^{2HH^+H^-}_{lm}\,,$$

and

$$\Gamma^{4H^+} = s^4_\beta\lambda_1 \,+\, c^4_\beta\lambda_2 \,+\, s^2_\beta c^2_\beta(\lambda_3+\lambda_4) \,+\, 2s^2_\beta c^2_\beta \mathrm{Re}\lambda_5 \,-\, 2s^3_\beta c_\beta \mathrm{Re}\lambda_6 \,-\, 2s_\beta c^3_\beta \mathrm{Re}\lambda_7\,. \quad (2.34)$$

The quantities g^{3H}_{ijk}, $g^{HH^+H^-}_i$, g^{4H}_{ijkl}, $g^{2HH^+H^-}_{ij}$ in (2.33) characterize the proper vertex corrections to the corresponding Higgs self-couplings. We observe that, exactly as is the case for Γ^{4H^+} in (2.34), all these newly-introduced couplings depend on the radiatively-corrected quartic couplings λ_1, λ_2, ..., λ_7. Their analytic forms are given in Appendix A.

3 Constraints on the CPX scenario from LEP searches

The OPAL Collaboration [29] has reported preliminary results on the search for Higgs bosons in the MSSM with explicit CP violation, taking the parameters to be those defined in the CPX scenario [6],

$$\begin{aligned} M_{\rm SUSY} \;&=\; \widetilde{M}_Q \;=\; \widetilde{M}_t \;=\; \widetilde{M}_b \;=\; 0.5\ \mathrm{TeV}\,, \quad \mu \;=\; 2\ \mathrm{TeV}\,, \quad |A_t| \;=\; |A_b| \;=\; 1\ \mathrm{TeV}\,, \\ |m_{\tilde B}| \;&=\; |m_{\tilde W}| \;=\; 0.2\ \mathrm{TeV}\,, \qquad |m_{\tilde g}| \;=\; 1\ \mathrm{TeV}\,, \end{aligned} \quad (3.35)$$

where $M_{\rm SUSY}$ is the characteristic third generation squark mass scale, and $m_{\tilde B}$, $m_{\tilde W}$ are the bino and wino masses, respectively.

OPAL presented exclusion regions in the M_{H_1}–$\tan\beta$ plane for different values of the CP-violating phases, assuming $\arg A_t = \arg A_b = \arg m_{\tilde g} = \phi_{\rm CPX}$, with $\phi_{\rm CPX} = 90^\circ, 60^\circ, 30^\circ$, and 0°. Quite generally, there is no reason to expect the equality of the phases of the trilinear scalar couplings and the gaugino masses, nor to assume that $\phi_{\rm CPX} \leq 90^\circ$, and our analysis departs from this assumption.

To reproduce the results of the OPAL analysis, we rely on the combined ALEPH-DELPHI-L3-OPAL (ADLO) results for the $ZH_{\rm SM}(\to b\bar b)$ channel [30] and the $hA \to 4b$ channel [31]. Although the experimental hA analysis has been done for approximately equal values of the masses of the neutral Higgs bosons h and A, there is no major loss in efficiency when the splitting between these masses becomes larger [32], and therefore it is safe to apply those limits to a more generic set of masses H_i, H_j in the CP-violating scenario.

Using the results of these experimental analyses, we have generated Figure 1, based on the CPX scenario with $M_{\rm SUSY} = 0.5$ TeV. In this plot, the light grey area covers the theoretically allowed region of parameter space (consistent with electroweak symmetry

breaking), the medium grey region shows the exclusion from ZH_i final states, the dark grey region is excluded by the search for $Z^* \to H_i H_j \to 4b$ final states, and the black region is excluded by both searches.

When comparing the results in Fig. 1 with the OPAL results [29], we note that our limits on $\tan\beta$ are somewhat stronger than the OPAL limits. This can be attributed to the fact that our analysis is based on combined ADLO limits obtained from all four experiments [31]. The results of our analysis show also a somewhat better reach than the OPAL one in the $H_i H_j$ production channel. This can again be attributed to our use of the combined results of all four experiments and the fact that, following the above discussion, we have assumed no deterioration of the $H_i H_j$ signal for $M_{H_i} \neq M_{H_j}$. We expect that our CPX estimates will be quite similar to the final LEP combined results.

We see from the cases displayed in Fig. 1 that the case of vanishing phases is most severely constrained by the LEP data. Most of the coverage arises from the ZH_1 or H_1H_2 processes. The appearance of two 'fingers' in the ZH_1 coverage at large $\tan\beta$ for vanishing phases arises from the shape of the LEP exclusion curve, which is distorted by a marginal excess in the region $m_h \sim 80 - 90$ GeV [30]. The case of phase 30° is very similar, and the 60° case has analogous features.

For significant values of the phases, there are regions of parameters in which the lightest neutral Higgs boson is very weakly coupled to the Z gauge boson, and light enough for the heavier neutral Higgs states to decay into a pair of H_1 bosons. In these regions of parameters, the heavier Higgs states decay into a final state containing four b quarks. Therefore, the dominant production and decay modes contain 6 jets in the final state. The current experimental strategy is to employ the standard 4-b analysis by forcing (with suitable jet definitions) the 6-jet topologies into 4-jet ones. This leads to a very low efficiency for the real 6-jet signal, and hence a significant region of CPX parameter space where light Higgs bosons may exist but are not excluded by the current analyses. In our analysis of the MSSM parameter space excluded by Higgs boson searches at LEP, we have not attempted to simulate the signatures associated with the decay of heavy neutral Higgs bosons into lighter ones. Nonetheless, we are hopeful that a dedicated 6-jet analysis could cover this region. Returning to Fig. 1, the upper two panels $(90°, 60°)$ demonstrate that LEP cannot exclude the presence of a light Higgs boson at $\tan\beta \sim 3 - 5, M_{H_1} \lesssim 60$ GeV and $\tan\beta \sim 2 - 3, M_{H_1} \lesssim 40$ GeV, respectively, in good qualitative agreement with the OPAL results. Using the ADLO data in the $ZH_i(\to b\bar{b})$ channel, a Higgs boson with the Standard Model coupling can be excluded if $M_{H_i} < 115$ GeV, and even a low-mass Higgs boson can be excluded if $|g_{H_i ZZ}| \gtrsim .22$ relative to the Standard Model coupling.

In Figs. 2 and 3, we have presented a generalization of the above analysis to unequal

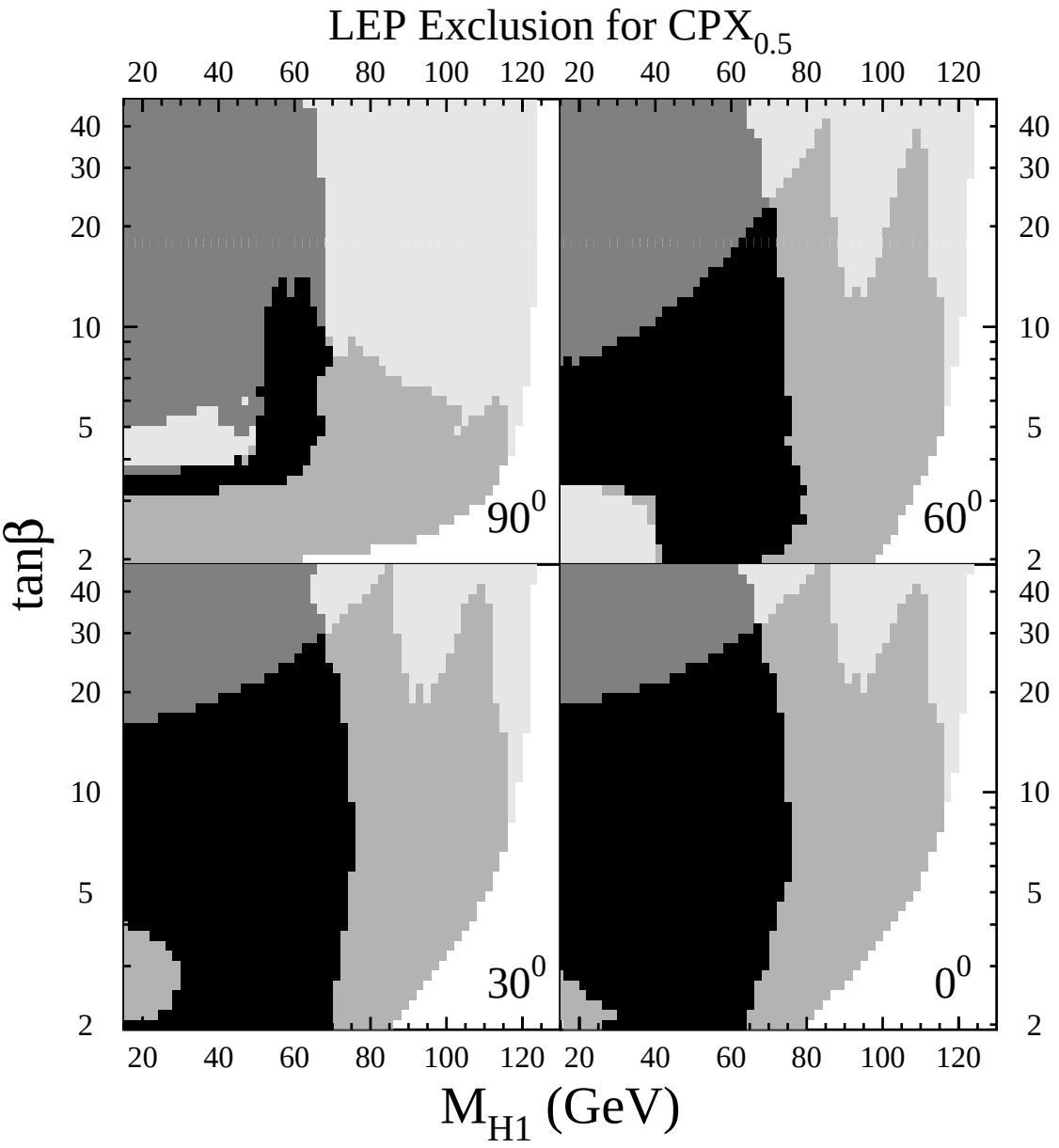

Figure 1: *Approximate LEP exclusion limits in the M_{H_1}–$\tan\beta$ plane for various CPX scenarios, using combined LEP results. The light grey covers all the region of parameter space that is consistent with electroweak symmetry breaking, the medium grey shows the exclusion from $e^+e^- \to ZH_i$, the dark grey shows the region excluded by $Z^* \to H_iH_j \to 4b$ searches, and the black region is excluded by both searches.*

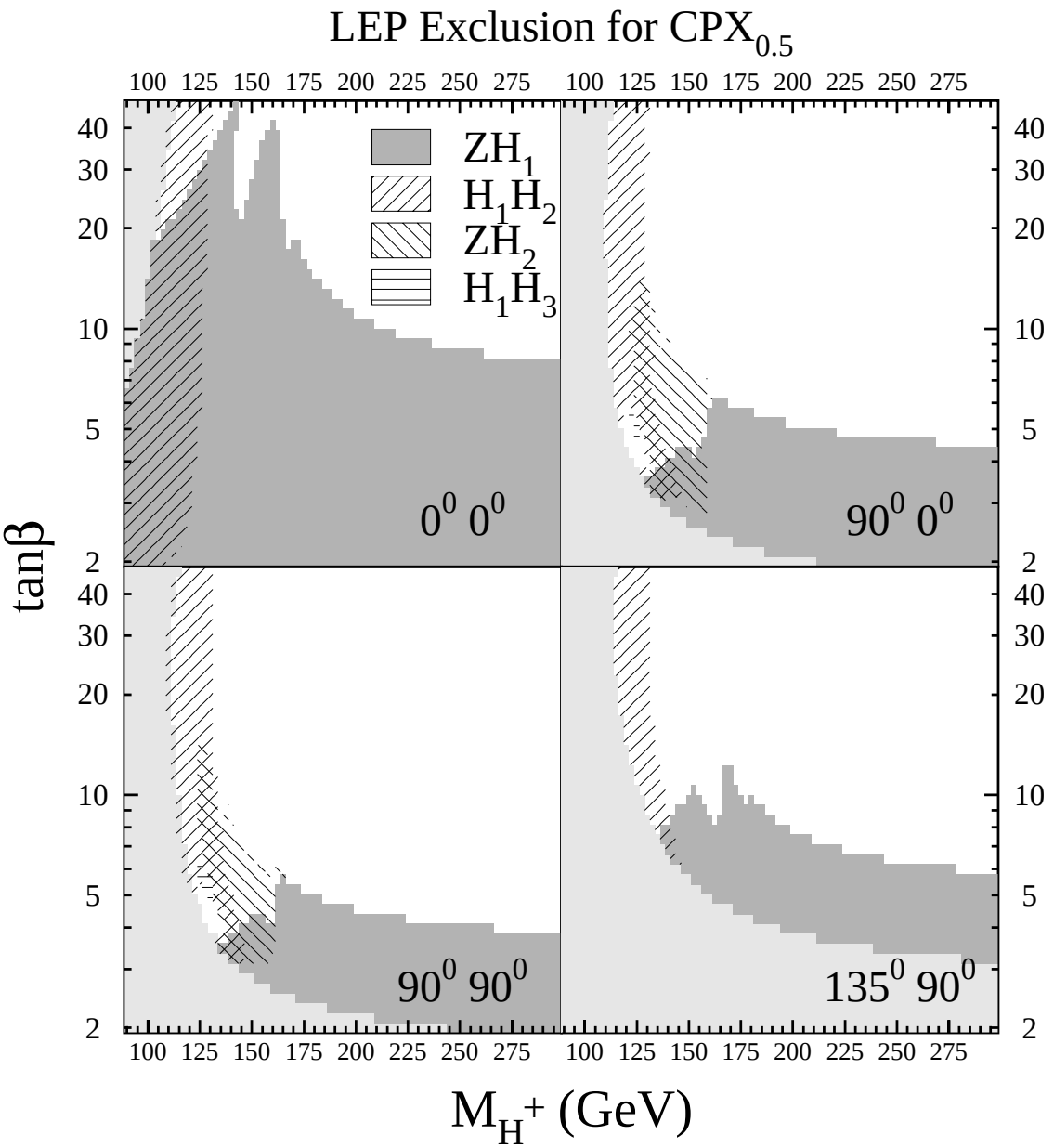

Figure 2: *LEP exclusion limits in the CPX benchmark scenario in the M_{H^+}–$\tan\beta$ plane for different values of the phases arg(A) and arg$(m_{\tilde{g}})$ of the trilinear couplings $A_{t,b}$ and the gluino mass parameter, respectively. The four panels show the results for (0,0); (90,0); (90,90) and (135,90) degrees, respectively. The light grey region is disallowed theoretically, the medium grey region is excluded by the absence of ZH_1, 45°-hatched region by the absence of H_1H_2, 135°-hatched region by the absence of ZH_2, and the horizontally-hatched region by the absence of H_1H_3.*

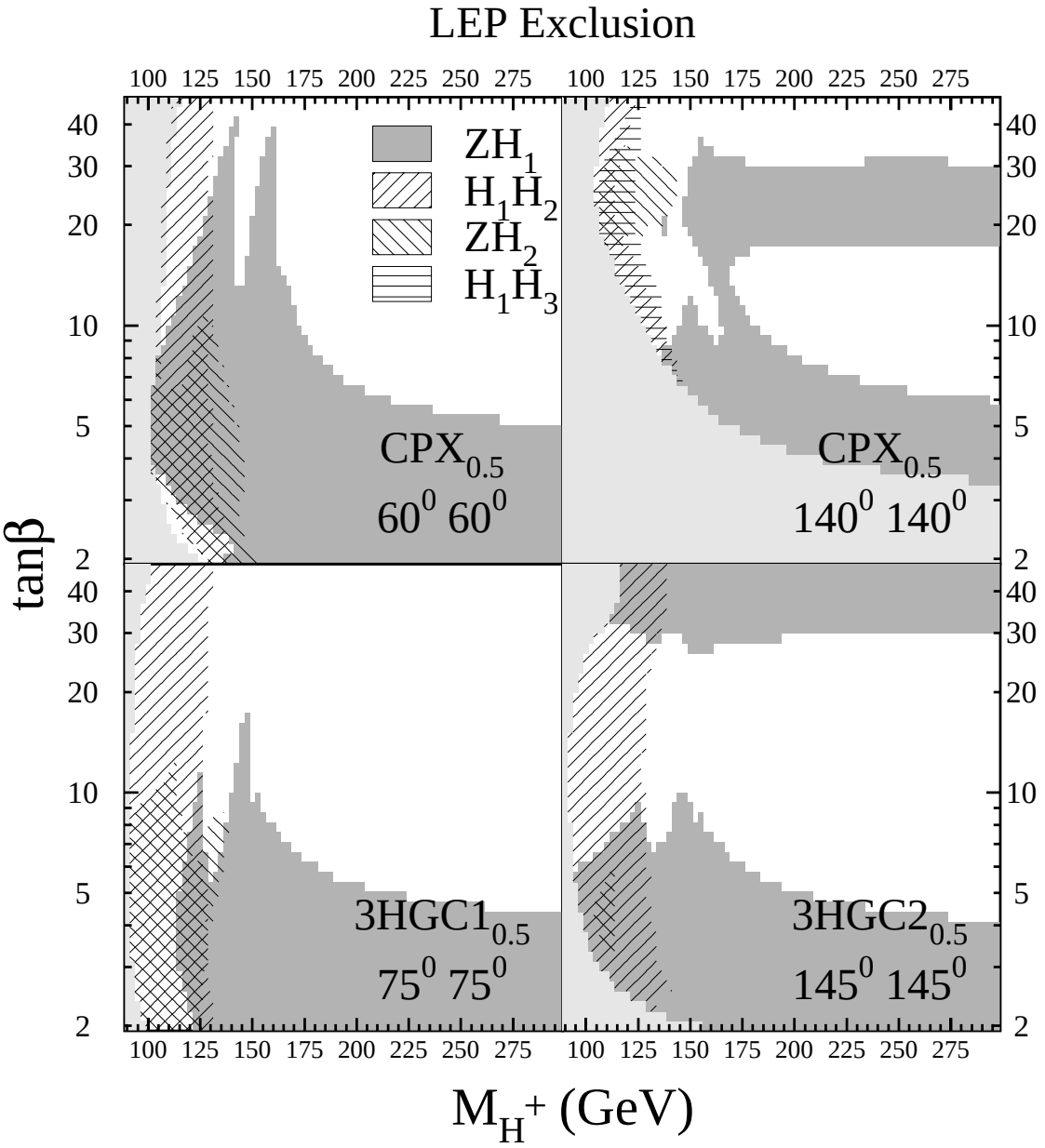

Figure 3: *Panels (a) and (b) are similar to Fig. 2, but for CP-violating phases (60,60) and (140,140) degrees. Panels (c) and (d) show two special scenarios 3HGC1 and 3HGC2, which are particularly challenging for all colliders: 3HGC1:* $M_{\rm SUSY} = 0.5$ *TeV,* $\bar{A} = 1.95$, $\bar{\mu} = 2.4$, *arg*$(A) = \arg(m_{\tilde{g}}) = 75°$*; 3HGC2:* $M_{\rm SUSY} = 0.5$ *TeV,* $\bar{A} = 2$, $\bar{\mu} = 2$, *arg*$(A) = \arg(m_{\tilde{g}}) = 145°$, $M_{\tilde{g}} = 0.5$ *TeV. The shadings and hatchings have the same significances as in Fig. 2.*

values of the CP-violating phases of the trilinear mass parameters $A_{t,b}$ and the gluino mass. The exclusion plots are presented in the M_{H^+}–$\tan\beta$ plane. For the case of equal values of the phases, these figures present analogous information to that presented in Fig. 1. Note the appearance of fingers for $\arg(A_{t,b}, m_{\tilde{g}})=(0^\circ, 0^\circ)$, as well as uncovered regions near $\tan\beta \sim 4-5$ and $M_{H^\pm} \sim 125-140$ GeV for $(90^\circ, 90^\circ)$, and near $\tan\beta \sim 2-3$ and $M_{H^\pm} \sim 105-130$ GeV for $(60^\circ, 60^\circ)$. Moreover, Figs. 2 and 3 show distinctively the regions covered by the different channels studied at LEP. The light grey regions of these figures are excluded theoretically, the medium grey regions are excluded by the absence of ZH_1, the regions hatched at 45° by the absence of H_1H_2, the regions hatched at 135° by the absence of ZH_2, and the horizontally-hatched regions by the absence of H_1H_3.

Fig. 2 is a study of the interplay of phases for the trilinear parameters $A_{t,b}$ and the gluino mass parameter. The appearance of substantial phases to the parameters can significantly modify the collider phenomenology (the phase of A_t providing the dominant effect). The addition of a phase to the gluino mass parameter, however contributes to CP-violating effects only at the two-loop level and its effect is comparatively smaller, as can be seen in Fig. 2. For the case of $\arg(A_{t,b}) = 90^\circ$, it is clear from Fig. 2 that, for $\tan\beta \simeq 4$–5, as the Higgs H_1 becomes lighter, it starts decoupling from the Z. There is a significant region of parameter space where, although heavier, H_2 is in the kinematic region accessible to LEP and couples relevantly to the Z gauge boson. For $M_{H^+} \lesssim 130$ GeV, H_1 becomes light enough that the decay $H_2 \to H_1H_1$ dominates over $H_2 \to b\bar{b}$, and therefore H_2 detection becomes difficult. Finally, for $\arg(A_{t,b}) = 135^\circ$ and $\arg(m_{\tilde{g}}) = 90^\circ$, and for moderate or large values of the charged Higgs mass, all neutral Higgs bosons rapidly become sufficiently heavy to be out of the reach of LEP for moderate and large values of $\tan\beta$.

In Fig. 3 we display results for the CPX scenario, for equal values of the $A_{t,b}$ and gluino mass phases equal to 60° and 140°. The region of parameters left uncovered by LEP for low values of $\tan\beta$ and of the charged Higgs boson mass, for phases equal to 60°, is seen more clearly than in Fig. 1. It is also apparent that, as happens for a CP-violating phase equal to 90°, close to the region left uncovered by LEP, there is a large region of parameters covered by the ZH_2 channel.

For phases equal to 140°, we find a peculiar behavior of the covered region of parameters for large values of the charged Higgs mass, which can be traced to the behavior of the H_1 mass shown in Fig. 4. For small and moderate values of $\tan\beta$, it has the standard behavior of the MSSM without explicit CP violation, increasing with $\tan\beta$. For $\tan\beta$ above about 10, however, it starts decreasing due to the effect of radiative corrections from the sbottom sector, which involve the bottom Yukawa coupling. The bottom quark Yukawa corrections are screened for sufficiently large values of $\tan\beta$, causing the mass of the H_1 to

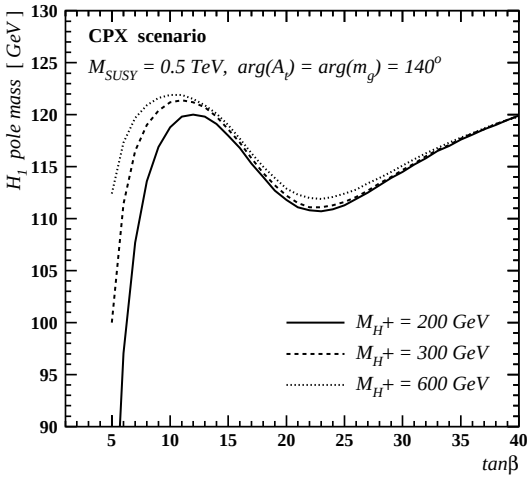

Figure 4: *The non-monotonic behavior of M_{H_1}, the mass of the lightest neutral Higgs boson, in the CPX scenario with arg(A_t) = arg($m_{\tilde{g}}$) = 140° for different values of M_{H^+}. The dip for $15 < \tan\beta < 30$ is due to the behavior of the radiative corrections from the sbottom sector, which are screened at large $\tan\beta$, as discussed in the text.*

increase again and eventually become larger than the LEP kinematic limit.

This screening phenomena occurs because the sbottom–induced radiative corrections are complex. At large values of $\tan\beta$, the bottom-quark Yukawa coupling h_b is approximately related to the bottom mass and to the Yukawa corrections Δh_b by

$$h_b = \frac{m_b}{v}\,\frac{\tan\beta}{1+(\Delta h_b/h_b)\tan\beta} \tag{3.36}$$

The negative corrections to the Higgs mass squared coming from sbottom loops are proportional to the fourth power of the modulus of h_b. For equal values of the phases of the gluino and of the trilinear mass parameter A_t, i.e. $\arg(A_t) = \arg(m_{\tilde{g}}) = \phi_{\rm CPX}$, the modulus of h_b is given by

$$|h_b| = \frac{m_b}{v}\,\frac{\tan\beta}{\sqrt{1+2|\Delta h_b/h_b|\cos(\phi_{\rm CPX})\tan\beta+\left(|\Delta h_b/h_b|\tan\beta\right)^2}} \tag{3.37}$$

For $\cos(\phi_{\rm CPX}) \geq 0$, the above expression is a monotonically increasing function of $\tan\beta$, meaning that the negative corrections induced by sbottom loops become larger for larger values of $\tan\beta$.

On the other hand, for negative values of $\cos(\phi_{\rm CPX})$, the expression for $|h_b|$ has a

maximum at a value of

$$\tan\beta^{\rm max} = -\frac{1}{|\Delta h_b/h_b|\cos(\phi_{\rm CPX})} \tag{3.38}$$

meaning that the negative effects on the Higgs mass induced by sbottom loops are most pronounced at intermediate values of $\tan\beta$, and are reduced again at large $\tan\beta$. For the particular case under consideration, we have $|\Delta h_b|/h_b \simeq 1/20$ and $\phi_{\rm CPX} = 140^\circ$, with $\cos(\phi_{\rm CPX}) \simeq 1/\sqrt{2}$, while $|h_b| \lesssim 1$ stays well within the perturbative range. Thus, lower values of the Higgs mass are obtained for $\tan\beta \simeq 25$ than for either smaller or larger values of $\tan\beta$. This feature is seen clearly in Fig. 4, and explains the stronger coverage of LEP at this intermediate region of $\tan\beta$, as seen in panel (b) of Fig. 3.

Apart from the above property, the only salient feature is that in the region between the one covered by LEP in the ZH_1 channel and that covered by LEP in the H_1H_2 channel, H_1 becomes light but couples very weakly to the Z boson.

The last two scenarios considered in Fig. 3 are interesting since, for moderate values of the charged Higgs mass of about 150 GeV, the three neutral Higgs bosons become quite similar in mass and share approximately equal couplings to the weak gauge bosons. We call these tri-Higgs-gauge coupling (3HGC) scenarios, which are denoted in short as 3HGC1 and 3HGC2. As we discuss below, the searches at hadron colliders become particularly difficult in 3HGC1 and 3HGC2. The excluded region for moderate and large values of the charged Higgs-boson mass and large values of $\tan\beta$ in the scenario 3HGC2 is related to the Higgs-sbottom coupling effect discussed above.

To summarize the results from LEP searches, the phenomenology is mainly sensitive to the values of g_{H_iZZ} and the kinematic limit on the Higgs boson masses. The exceptions are the cases when the decay $H_2 \to H_1H_1$ becomes relevant at small $\tan\beta$ and when radiative corrections extend the LEP coverage for certain choices of phases $\phi_{\rm CPX}$ at large $\tan\beta$. A Higgs boson with the Standard Model coupling can be excluded if $M_{H_i} < 115$ GeV, and even a low-mass Higgs boson can be excluded if $|g_{H_iZZ}| \gtrsim .22$ relative to the Standard Model coupling. Note that the application of the ZH_i and H_iH_j results to the CPX scenarios treats each potential signature independently. Any possible complications from one potential signal effecting the background estimate for another (and *vice versa*) are ignored. We are not aware of any experimental analysis of such a situation.

4 Higgs Boson Searches at Hadron Colliders

Experiments at the Tevatron and LHC will probe the MSSM Higgs sector beyond the kinematic and dynamical reach of LEP. At these hadron colliders, we have considered

several channels for Higgs boson H_i searches, where H_i stands for $H_{1,2,3}$:

(a) $t\bar{t}H_i(\to b\bar{b})$ at the LHC

(b) $W/ZH_i(\to b\bar{b})$ at the Tevatron

(c) $WW \to H_i(\to \tau^+\tau^-)$ at the LHC

(d) $gg \to H_i \to \gamma\gamma$ at the LHC.

In the absence of reliable experimental simulations, as in the case of LEP, we have not modified our analysis to account for the decay $H_j \to H_iH_i \to 4b$ $(j > i)$, should it become relevant. The search channels $(a) - (d)$ are considered to be the most promising for observing a Standard Model Higgs boson, and have been the most thoroughly analyzed and simulated. Since the MSSM Higgs sector has a decoupling limit, where there is a light Higgs boson with properties almost indistinguishable from a SM Higgs boson, it is appropriate to apply these SM analyses to the MSSM case. However, one would have to be careful in interpreting a signal in some of these channels. For example, signature (d) may arise when H_i is replaced by a pseudo-Goldstone boson, as in Technicolor models. Signature (a) may arise, for example, when H_i is replaced by a top-pion, as in a Topcolor model. Only observation of channels (b) and (c) would clearly indicate that the scalar H_i is associated with EWSB. Signature (a) may indicate that the scalar responsible for EWSB also generates fermion masses. Nonetheless, if signature (a) or (d) were observed with the rate expected in a weakly–coupled theory, it could be considered strong evidence for a fundamental Higgs scalar or scalars. In the present work, we do not analyze those signatures associated with non–SM–like Higgs bosons, such as charged Higgs or pseudoscalar Higgs bosons, since their interpretation would be ambiguous.

Figure 5 shows the coverage of the M_{H_1}–$\tan\beta$ plane by the Tevatron $W/ZH_i(\to b\bar{b})$ search (45° lines) and the combined LHC coverage for the $t\bar{t}H_i(\to b\bar{b})$, $WW \to H_i(\to \tau^+\tau^-)$ and $gg \to H_i(\to \gamma\gamma)$ searches (135° lines) for the same values of the CP-violating phases as chosen in Fig. 1. For the Tevatron, we show the 3σ evidence coverage with 5 fb^{-1}, while, for the LHC, we show the 5σ discovery coverage for the $\gamma\gamma$ and $b\bar{b}$ channels with 100 fb^{-1} and the $\tau^+\tau^-$ channel with 30 fb^{-1}. The previous LEP 95% C.L. exclusion is also included (medium grey) superimposed on the theoretically allowed region (light grey). While the Tevatron and LHC searches are adequate for extending the coverage into the large-$\tan\beta$ region, the region of small M_{H_1} and low $\tan\beta$ for $\phi_{\rm CPX} = 90°, 60°$ remains uncovered. Although the persistence of these regions can be clearly traced to the decay of the heavier Higgs bosons into lighter ones, one could inquire why the LHC cannot see the *lighter* Higgs

boson in the $t\bar{t}H_1$ and/or the gluon fusion channels. The reason is that, in the same region of parameters, H_1 couples weakly to the top quark, as well as negligibly to W and Z bosons. Therefore, not only is the $t\bar{t}H_1$ production channel suppressed but the loop-induced gluon fusion production and decay into photons is suppressed as well. Furthermore, since $\tan\beta$ is small, H_1 would likely not be observed in the pseudoscalar Higgs channel $b\bar{b}H_1(\to b\bar{b})$.

If, contrary to our expectations, a dedicated LEP analysis cannot cover this problematic region, there still remains the possibility of observing $H_2 \to H_1H_1$ decays (when H_2 is otherwise SM–like) at hadron colliders. Since H_2 is SM–like, there still is a substantial production cross section. Dedicated searches *should* be able to identify $4b$ final states with high efficiency and substantially less background than for the $2b$ case. Various cases of Higgs pair production, such as $gg \to H \to hh/AA$, have been considered in previous studies for the Tevatron and LHC, but mostly at the parton level [33, 34]. The studies would have to be updated for the case of explicit CP violation. Searches for $W/ZH_2(\to 4b)$ or $t\bar{t}H_2(\to 4b)$ may be more promising, if only because of the reduced backgrounds from requiring the leptonic decay of a W boson.

Outside these small regions of parameters, the search for neutral Higgs bosons at the Tevatron and LHC colliders are complementary and sufficient to cover the full parameter space in one or several channels. The Tevatron does not provide any additional coverage alone over all three LHC search channels. However, if we just focus on the W/ZH_i and $WW \to H_i$ channels – the only two which are dependent on the coupling g_{H_iWW} – then both are nearly sufficient to cover the entire parameter space: for 90°, $M_{H_1} \sim 80$ GeV and $\tan\beta \sim 10$, a small region is left uncovered without $t\bar{t}H_i$. This complementarity reflects the different production and decay channels that are being used in the search for neutral Higgs bosons, and is similar to that in the CP-conserving scenario [25]. For instance, there are regions of parameter space where either the $b\bar{b}$ or the $\tau^+\tau^-$ decay branching ratio of the lightest neutral Higgs boson is suppressed with respect to the Standard Model ones, while the other neutral Higgs bosons are heavy and weakly coupled to the gauge bosons. These suppressions tend to occur for large values of $\tan\beta$. The large values of μ chosen in our examples maximize the CP-violating effect, but also determine that for large values of $\tan\beta$ the quantum corrections to the bottom Yukawa coupling are large and sizeable, causing a visible displacement of the regions of suppressions of each coupling. Since, for a light enough Higgs, these two branching ratios tend to be very important, a suppression of one of them tends to enhance the other. We discuss specific examples below. For smaller values of μ, both the $b\bar{b}$ and $\tau^+\tau^-$ couplings can be suppressed simultaneously and then the $\gamma\gamma$ decay branching ratio of the lightest Higgs boson tends to be enhanced. An analysis of these cases can be found in Ref. [25].

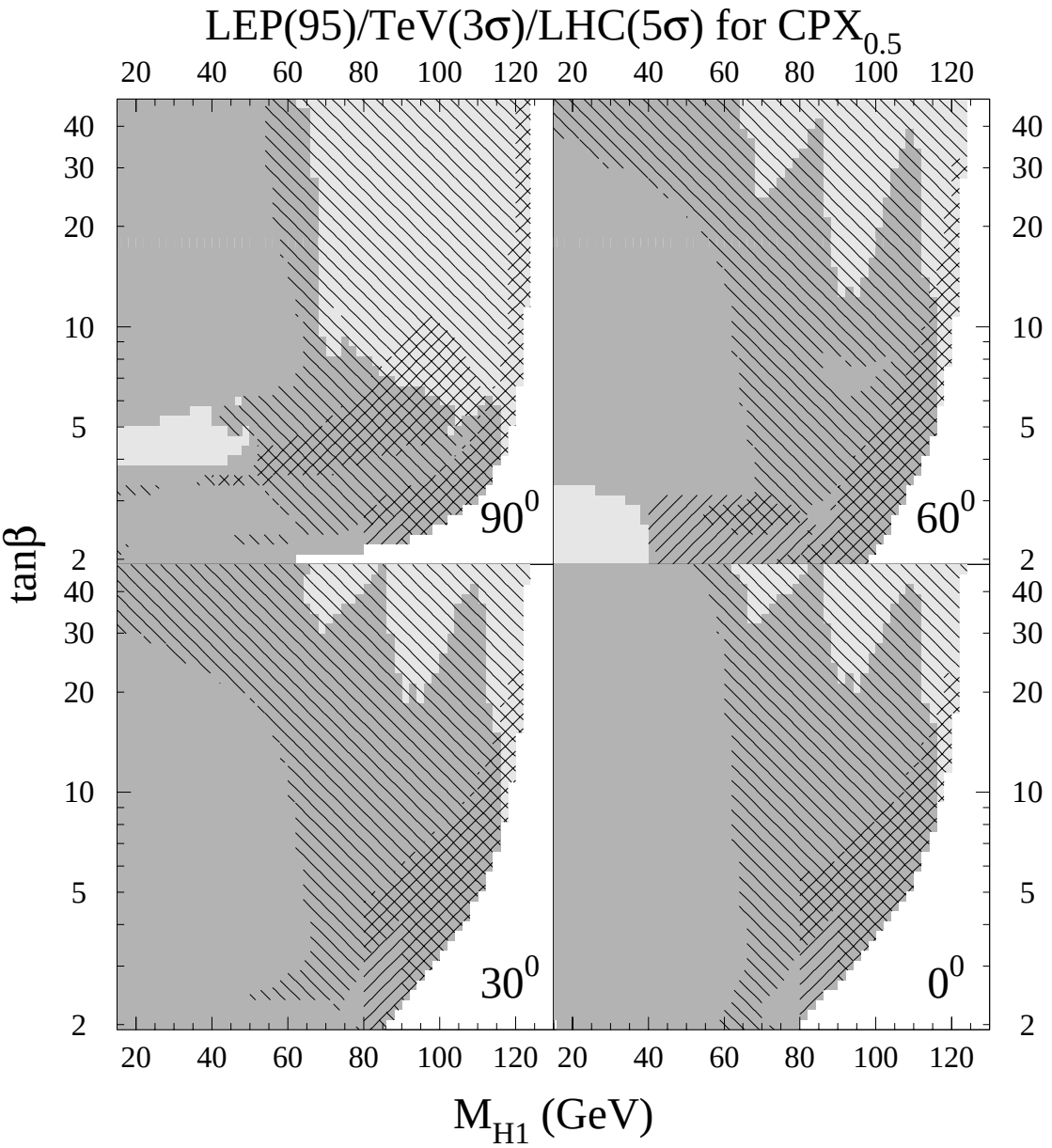

Figure 5: *Approximate Tevatron/LHC discovery and LEP exclusion limits in the* M_{H_1} – $\tan\beta$ *plane for the CPX scenario with both phases set to: (a)* $90°$*, (b)* $60°$*, (c)* $30°$*, and (d)* $0°$*. The reach of the Tevatron* $W/ZH_i(\to b\bar{b})$ *search is shown as* $45°$ *lines and that of the combined LHC search channels as* $135°$ *lines.The combined LEP exclusion is shown in medium gray, superimposed on the theoretically allowed region in light grey.*

4.1 Detailed Analysis of the different scenarios

In Figs. 6–13, we present a detailed analysis of the regions covered by the relevant search channels at the Tevatron and at the LHC. In each of these Figures, the four panels display the regions for which Higgs bosons may be discovered at the 5-σ level at the LHC via the $t\bar{t}H_i$ channel with 100 fb^{-1} (two darkest shades of grey) and 30 fb^{-1} (135° lines) the weak-boson-fusion channel using 30 fb^{-1} (two darkest shades of grey) and the gluon fusion channel with $H_i \to \gamma\gamma$ using 100 fb^{-1} (two darkest shades of grey) and 30 fb^{-1} (135° lines), as well as the region for which the Tevatron can provide 3-σ evidence with 5 fb^{-1} (two darkest shades of grey) and 2 fb^{-1} (135° lines) of integrated luminosity. In each case, the darker shade of grey extends beyond the LEP exclusion. The 3-σ coverage with 5 fb^{-1} at the Tevatron is very similar to the region that would be obtained for 5-σ discovery with 15 fb^{-1}, or for 95% C.L. exclusion with 2 fb^{-1}. The reason why we have only analyzed 30 fb^{-1} in the case of weak-boson fusion is that a realistic analysis exists only for moderate instantaneous luminosity, and detection in this channel might be compromised in the different environment created by high-luminosity LHC running. For the Tevatron, we chose to present results that can simultaneously indicate the Higgs discovery potential under a conservative assumption of the total integrated luminosity (5 fb^{-1}), for which only a 3-σ evidence may be obtained in the regions not excluded by LEP. This can be directly compared to a more optimistic assumption (15 fb^{-1}), for which discovery may be possible well beyond the region of parameters covered by LEP. Finally, in all the scenarios studied, there are regions where at least two Higgs bosons are close in mass and have similar strength couplings to W/Z bosons. Our prescription is to add the signals from $H_i \to b\bar{b}$ and $H_i \to \tau^+\tau^-$ with no degradation if the mass difference is less than 5 GeV (which is substantially smaller than the expected mass resolution), otherwise the signals are treated separately. We discuss this more later. Because of the precision electromagnetic calorimetry expected at the LHC, we do not combine $H_i \to \gamma\gamma$ signatures, though this is of little practical consequence.

Figure 6 demonstrates the case of vanishing phases. Because the CPX scenario has large values for μ and $m_{\tilde{g}}$, there is a large value for the supersymmetric loop corrections to the b-quark Yukawa coupling from (2.4, 2.5). Furthermore, since $\mathrm{sgn}(\mu m_{\tilde{g}}) > 0$, the b quark Yukawa coupling is decreased relative to the τ lepton Yukawa coupling. The right lobe of the $t\bar{t}H_i$ coverage (a) arises from $H_i = H_1$, with a transition to H_2 and then H_3 in the left lobe. The suppression of the $b\bar{b}$ coupling relative to $\tau^+\tau^-$, in conjunction with the sharing of the $g_{H_i\bar{t}t}$ coupling between (in this case) two Higgs bosons, results in the dip near $M_{H^\pm} \sim 150$ GeV. For this case without explicit CP violation, that region corresponds exactly to $M_A \sim m_h^{\max}$, where $m_h^{\max}$ is the maximal value of the Standard Model–like Higgs

boson in the decoupling limit. Because of the enhanced $\tau^+\tau^-$ coupling relative to $b\bar{b}$, the $WW \to h$ channel (c) does not exhibit this phenomena. For $\tan\beta >$ a few, the W/ZH_i channel (b) has a similar behavior as $t\bar{t}H_i$. The limited coverage from the $h \to \gamma\gamma$ channel (d) is a common feature of all the scenarios we have studied. Even when $g_{H_iWW} \sim 1$, a suppression of BR($h \to \gamma\gamma$) occurs because $g_{H_i\bar{b}b}$ is enhanced over the SM value. The large values of $|\mu|$ and $|A|$ necessary to cause substantial effects typically increased the off-diagonal elements of the 3×3 Higgs squared–mass matrix relative to the diagonal elements. Note that the $WW \to H_i(\to \tau^+\tau^-)$ channel with 30 fb^{-1} is sufficient alone to cover the $M_{H^\pm}$–$\tan\beta$ plane. With the same integrated luminosity, neither the $t\bar{t}H_i$ nor the $H_i \to \gamma\gamma$ channels even extend *beyond* the LEP coverage. Of course, the former is a discovery region, whereas the latter is only 95% C.L. exclusion.

Another possible variant on the CPX scenario is to introduce CP violation to the Higgs sector through a substantial phase for $m_{\tilde{g}}$, $\phi_{\tilde{g}} = 90^\circ$ (not shown). The primary effect is to decrease the suppression of $g_{H_i\bar{b}b}$ relative to $g_{H_i\tau\tau}$, but, as discussed before, the gluino phase effects are quite mild.

The introduction of a phase for $A_t = A_b$ allows for CP-violation effects at small values of $\tan\beta$, as shown in Fig. 7. As discussed previously, it is now possible for the lightest Higgs boson H_1 to become quite light and have a negligible coupling to vector bosons. Furthermore, the decay $H_2 \to H_1H_1$ becomes kinematically possible, introducing a region that remains uncovered by all experiments if one considers only the detailed analyses performed so far. Another region of difficult coverage appears in the $t\bar{t}H_i(\to b\bar{b})$ channel, for a charged–Higgs mass close to 125 GeV. This did not occur for vanishing phases, and only arises now because of the transition away from the region where $H_2 \to H_1H_1$ occurs when H_2 has a substantial coupling to the Z boson. This does not occur for weak boson fusion in the $H_i \to \tau\tau$ channel because of the enhancement of the τ coupling over that of the b. In this region of parameters, the coupling of H_1 and H_2 to the top quark and weak bosons is somewhat suppressed, though H_2 is relatively more strongly coupled to these particles than H_1. Due to finite quantum corrections, the ratio of branching ratios BR($H_1 \to b\bar{b}$)/BR($H_1 \to \tau\tau$) is suppressed with respect to the Standard Model value. The substantial increase in BR($H_2 \to \tau\tau$) means that $H_2 \to \tau\tau$ can still be observed, even though its vector–boson coupling is suppressed. Indeed, H_2 is also visible in the channel $t\bar{t}H_2$ in a small region of parameters, for somewhat larger values of the charged Higgs mass.

We show in Fig. 8 the effect of including a gluino phase as well, which, as mentioned before, does not change significantly the picture, apart from the fact that small regions of uncovered parameter space appear. Those uncovered regions appear for a charged–Higgs mass around 130 GeV (160 GeV) because two of the Higgs bosons, H_3 and H_2 (H_1 and

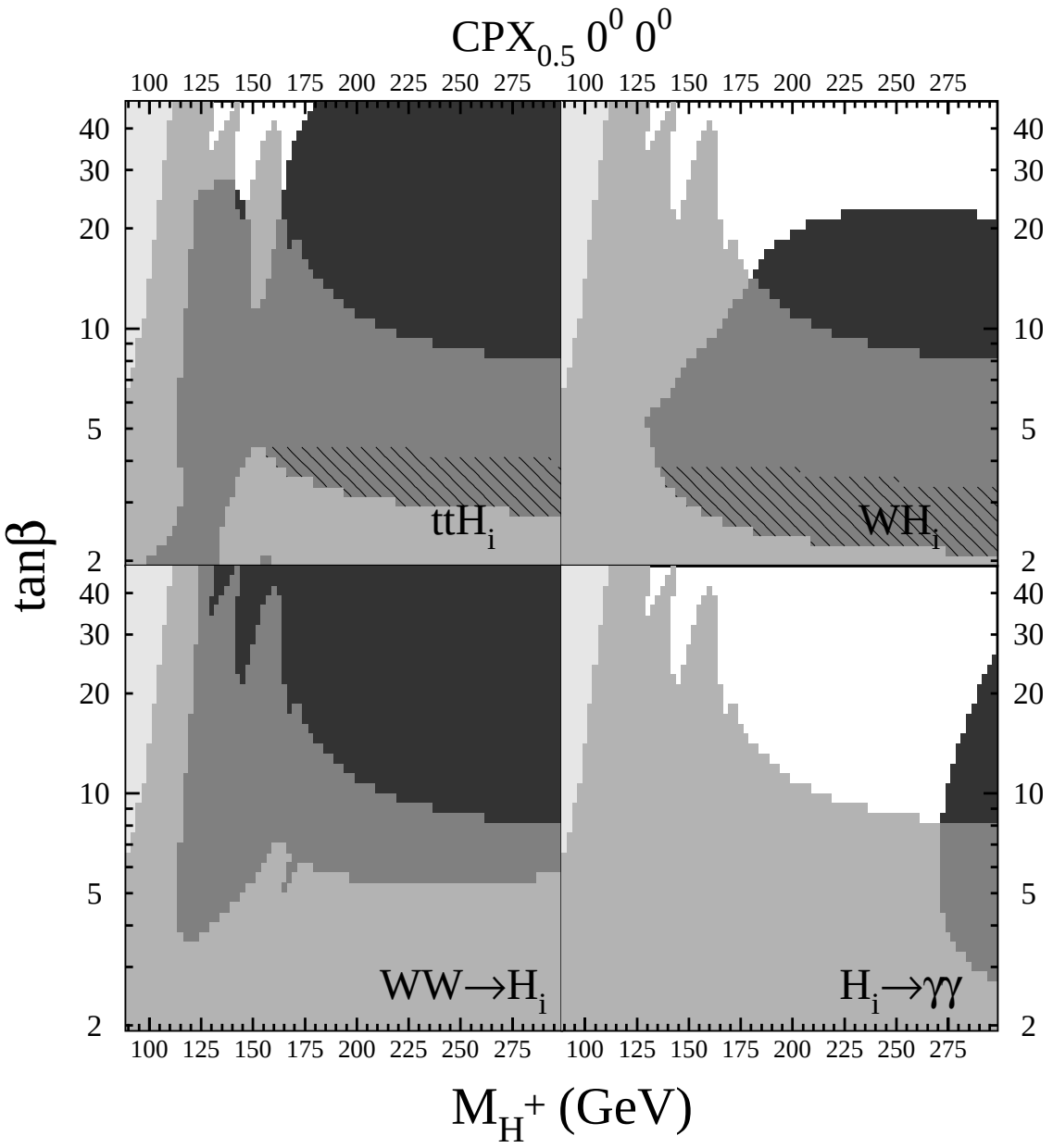

Figure 6: *Coverage of the $M_{H^\pm}$–$\tan\beta$ plane in the CPX scenario with $M_{\rm SUSY} = 0.5$ TeV and for the phases shown at top. The light grey region is theoretically excluded, and the two medium grey regions are excluded by LEP . The two darkest shades of grey are (a) the 5-σ discovery region at the LHC using $t\bar{t}H_i \to b\bar{b}$ (100 fb^{-1}); (b) the 3-σ evidence region at the Tevatron using $W/ZH_i \to b\bar{b}$ (5 fb^{-1}); (c) the 5-σ discovery region at the LHC using $WW \to H_i \to \tau^+\tau^-$ (30 fb^{-1}); and (d) the 5-σ discovery region at the LHC using $H_i \to \gamma\gamma$ with 100 fb^{-1} of luminosity. The 135° lines in panels (a), (b), and (d) show the coverage for 30, 2, and 30 fb^{-1} of data, respectively. This baseline model shows the behavior when no CP violation is present, i.e., the phases of $A_t = A_b$ and $m_{\tilde{g}}$ are both zero.*

H_2) are separated in mass (greater than 5 GeV apart) and share equal couplings, of order a half of the SM values, to the weak bosons and the top quark.

An interesting feature appears for the case displayed in Fig. 9. For moderate and large values of the charged–Higgs mass and large values of $\tan\beta \gtrsim 30$, the lightest Higgs–boson mass is about 123 GeV. For these values of the Higgs mass, discovery in the weak-boson fusion process demands a slightly larger branching ratio into τ leptons than in the SM. This occurs for smaller values of the charged–Higgs mass, but as the charged–Higgs mass increases the branching ratio into τ leptons becomes smaller than the SM one, and remains like this until the decoupling limit. The $b\bar{b}$ decay branching ratio has a different behavior, as we see in the panel showing the expected Tevatron coverage. The mass M_{H_1} is about 123 GeV in the large-$M_{H^\pm}$, large-$\tan\beta$ limit, but BR($H_1 \to b\bar{b}$) is slightly larger than in the SM, explaining the appearance of coverage in that region; the lack of coverage starting near $M_{H^\pm} \sim 235$ GeV and $\tan\beta \sim 20$ reflects the difficulty of establishing evidence for a SM Higgs boson of mass 123 GeV. As usual, for larger values of the charged–Higgs mass, the $\gamma\gamma$ mode becomes relevant as a discovery channel, since the search for a Standard Model Higgs boson is efficient. Note also the disappearance of an uncovered region associated with $H_2 \to H_1 H_1$.

The case of phases equal to 60°, displayed in Fig. 10, is similar to the case of 90°, although the asymptotic value of the H_1 mass is somewhat lower. Most of the features of the Higgs searches in these two cases have similar behaviors, though occurring for different parameters, so we do not expand on them further.

Our final example for the CPX scenario has phases equal to 140°. In this case, unlike the other examples, there is a relative suppression of the τ branching ratio of H_1 in large fractions of the parameter space, which explains the large regions of parameter space uncovered by the weak-boson-fusion process. This search channel becomes efficient whenever the Higgs mass is at the limit of the LEP reach, since in this case only a lower decay branching ratio is sufficient, as seen in Table 3 of Appendix B. For slightly shifted values of $M_{H^\pm}$ and $\tan\beta$, instead the $b\bar{b}$ coupling is suppressed relative to $\tau^+\tau^-$. The complementarity of these channels is clearly illustrated in panels (b) and (d).

One interesting phenomena that arises in the CPX scenario, which is experimentally challenging, is the appearance of regions uncovered because of $H_2 \to H_1 H_1$ decay. As noted previously, there are regions where two Higgs bosons share the coupling to W/Z bosons and $t\bar{t}$, but are separated in mass. In this 'transition region' from one Higgs boson being most SM–like to another one, the effective signal is halved. In the MSSM without explicit CP violation, these Higgs bosons are nearly degenerate in mass, and they are most likely indistinguishable from two Higgs bosons with the experimental resolution. After

including explicit CP violation, the mass splittings can be significantly larger, and all three Higgs bosons can share the W/Z coupling. We present here only two example scenarios that exhibit this phenomena – many more are possible. Under our prescription for adding signals occurring at masses within 5 GeV, the last two scenarios analyzed in Figs. 12 and 13 show small regions of parameters uncovered by any of the colliders. The size of these uncovered regions may be underestimated. Since there are potentially 3 Higgs bosons yielding a similar signature in these regions, and one may have to rely on experiment to normalize the background, the Higgs signal may be entirely washed out. Consider, for example, the expected number of signal and background events for the $\tau^+\tau^-$ channel shown in Table 3. Since $S/B \gg 1$, the accumulation of signals in nearby bins could substantially increase the background estimate. Clearly, the possibility that Higgs bosons may provide backgrounds for the other Higgs bosons should be understood and analyzed in more detail.

On the other hand, one consequence of sharing the coupling to W and Z bosons is that all three neutral Higgs bosons may be observable at hadron colliders in the W/ZH_i and/or $WW \to H_i$ channels. This is an exciting possibility, since it would indicate that a 2HDM without explicit CP violation is inadequate to describe the data. We find no such overlap of 5-σ signatures from all three neutral Higgs bosons in these channels for the scenarios presented here. Furthermore, using the expected reach of the ATLAS collaboration for the $gg \to H_{\rm SM} \to ZZ^* \to 4\ell$ channel [34], we have checked that there is almost no coverage beyond LEP for observing even a single Higgs boson.

5 Conclusions

We have presented in this article a phenomenological analysis of Higgs boson searches in Standard Model channels at the Tevatron collider and the LHC, for the case of the MSSM with explicit CP violation. We have also provided analytical expressions for the effective couplings of the neutral and charged Higgs bosons to fermions and to gauge bosons and the Higgs-boson self couplings within the MSSM with explicit CP violation. These expressions have been incorporated in the program `CPHDECAY` [19], used to perform our analysis.

After considering the LEP limits and comparing our results with the published LEP analyses, we have analyzed the reach of the Tevatron collider and the LHC in the Standard Model search channels for a neutral Higgs boson in the CPX scenario, as well as in other interesting scenarios. Our study was motivated by the fact that the latest LEP data prove insufficient to exclude a light MSSM Higgs boson in the CPX scenario, with a mass smaller than 60–70 GeV. Further coverage of the MSSM parameter space with CP-violating phases

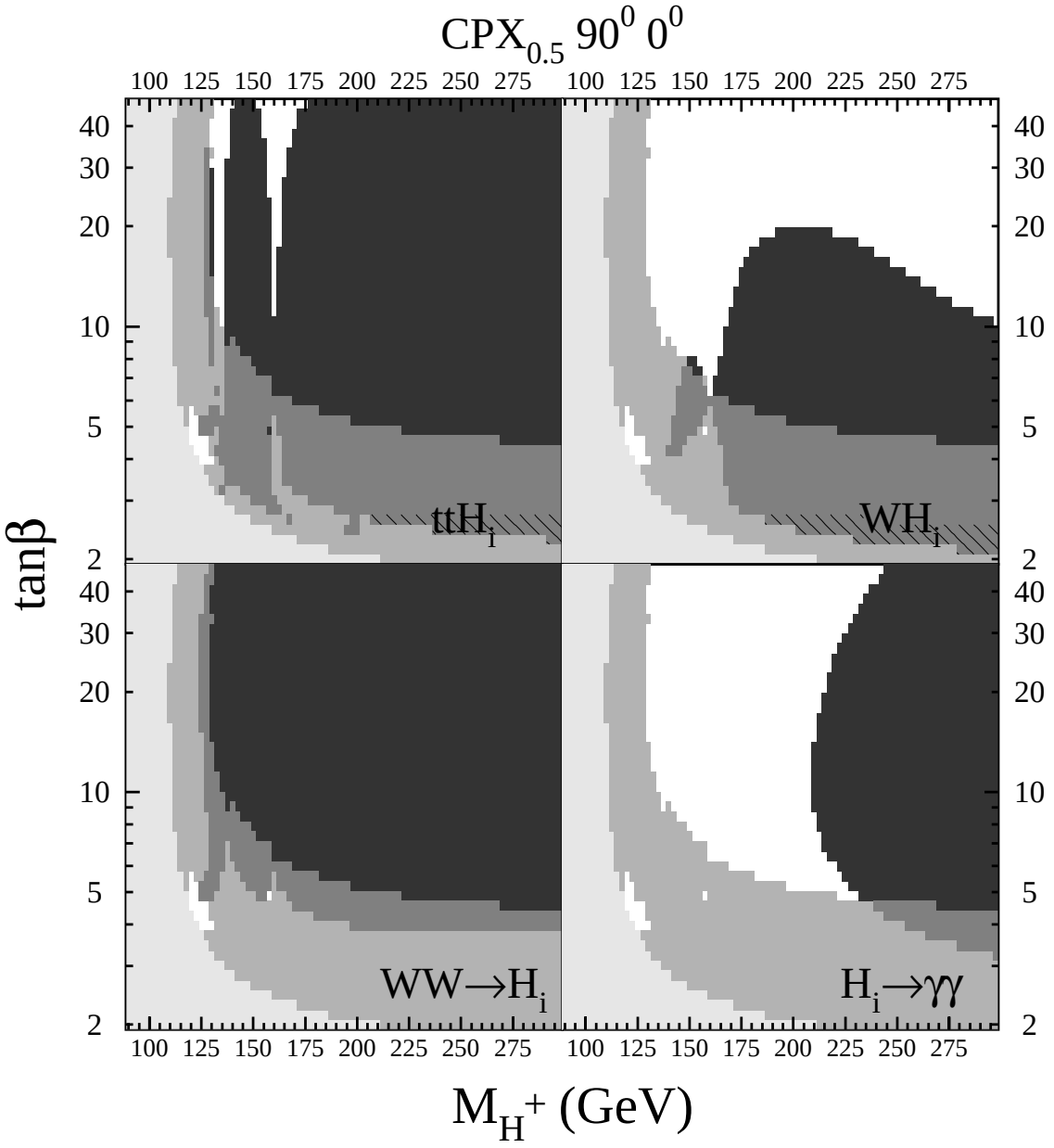

Figure 7: *Same as Fig. 6, but for CP-violating phases (arg($A_{t,b}$), arg($m_{\tilde{g}}$)) = ($90^\circ, 0^\circ$).*

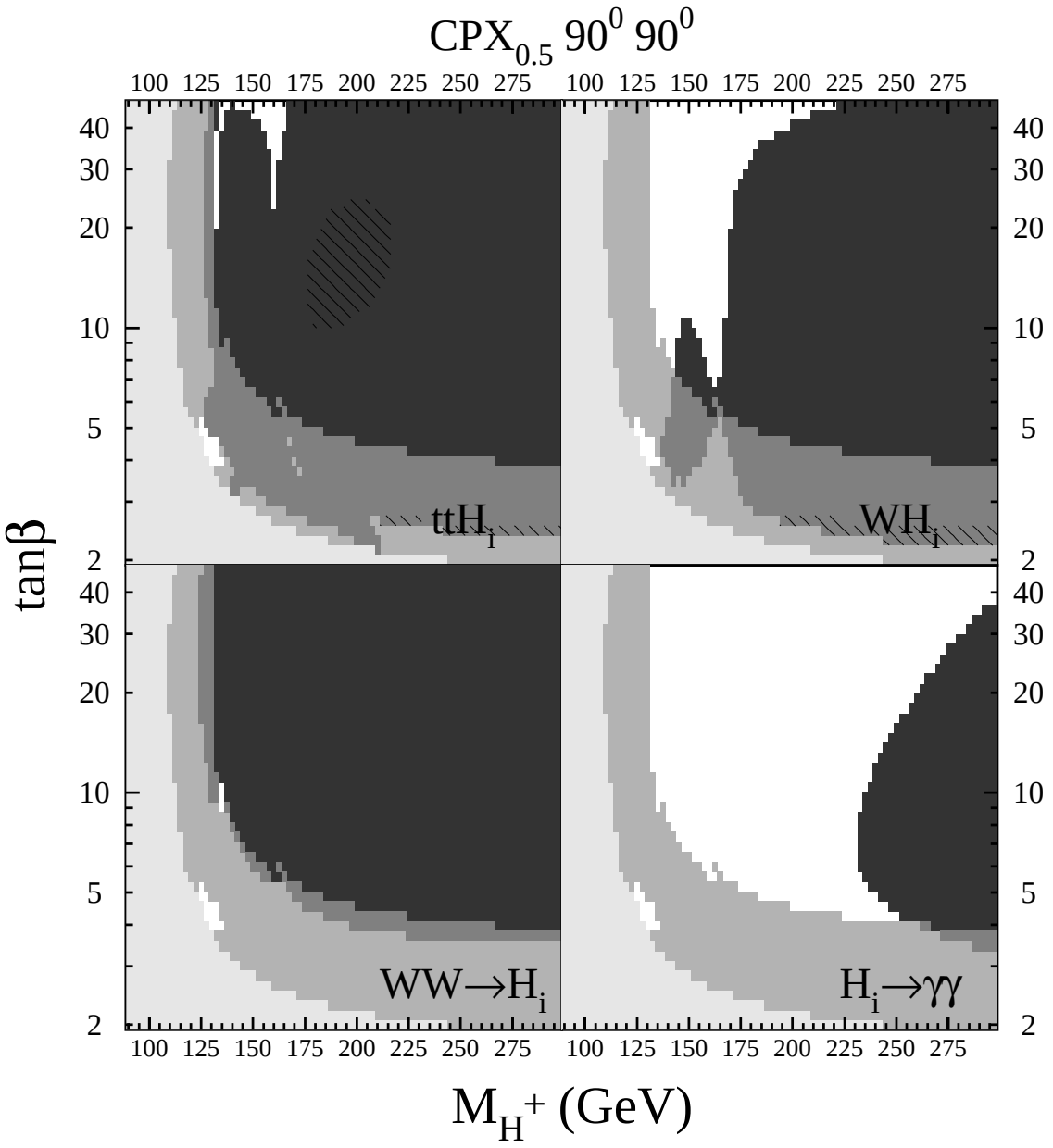

Figure 8: *Same as Fig. 6, but for CP-violating phases* $(arg(A_{t,b}),\ arg(m_{\tilde{g}})) = (90°, 90°)$.

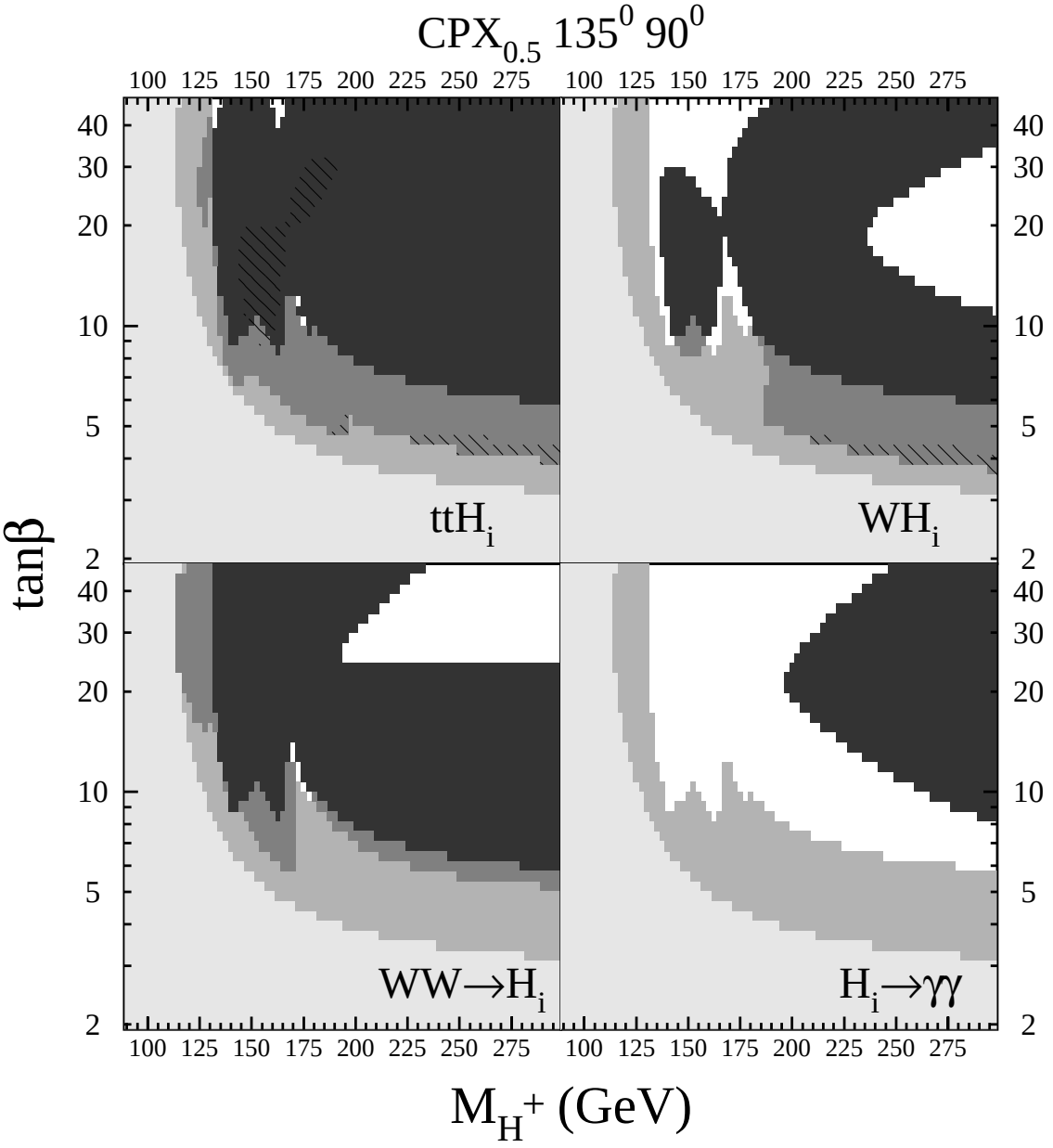

Figure 9: *Same as Fig. 6, but for CP-violating phases (arg($A_{t,b}$), arg($m_{\tilde{g}}$)) = (*$135^\circ, 90^\circ$*).*

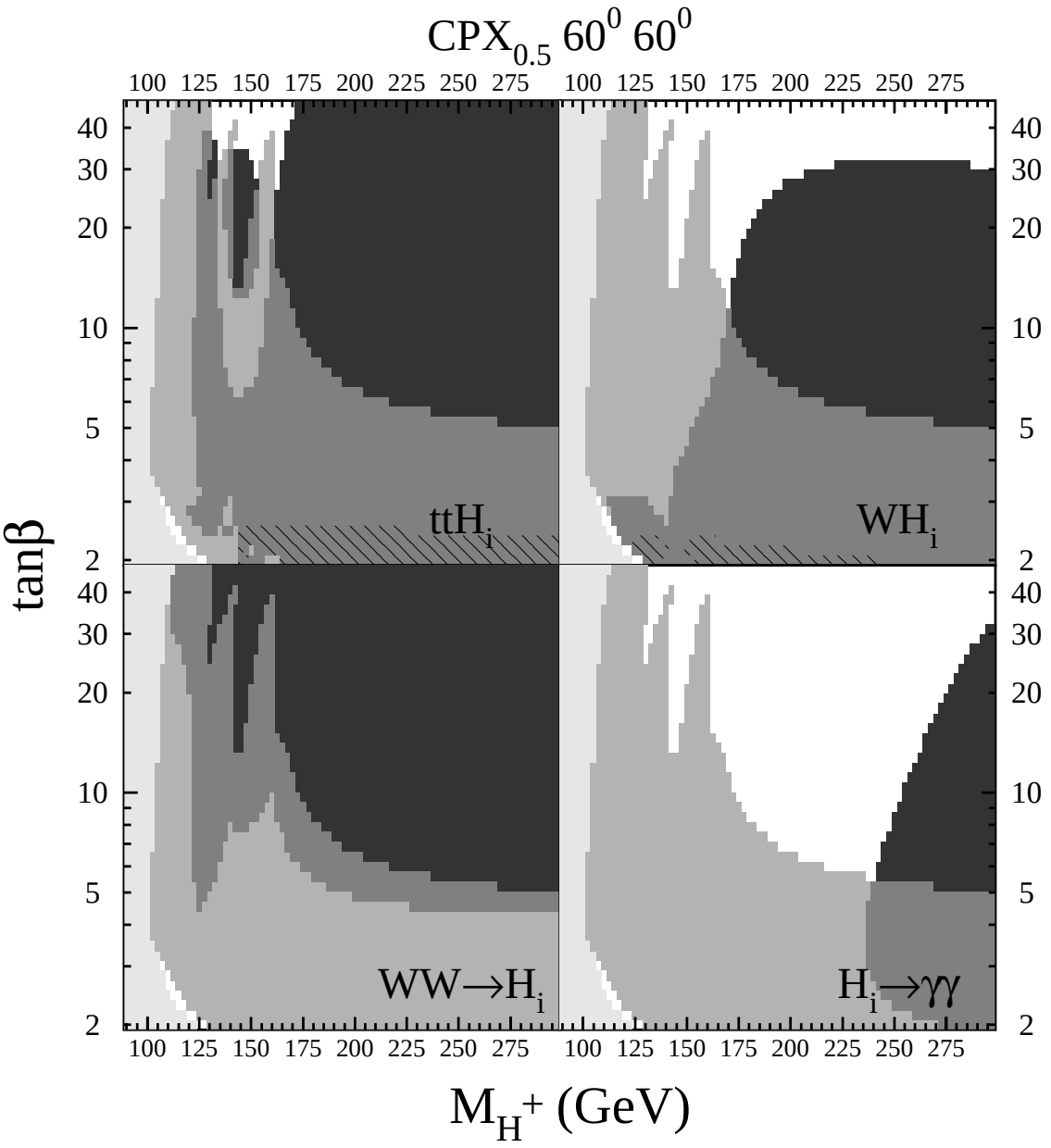

Figure 10: *Same as Fig. 6, but for CP-violating phases (arg($A_{t,b}$), arg($m_{\tilde{g}}$)) = ($60^\circ, 60^\circ$).*

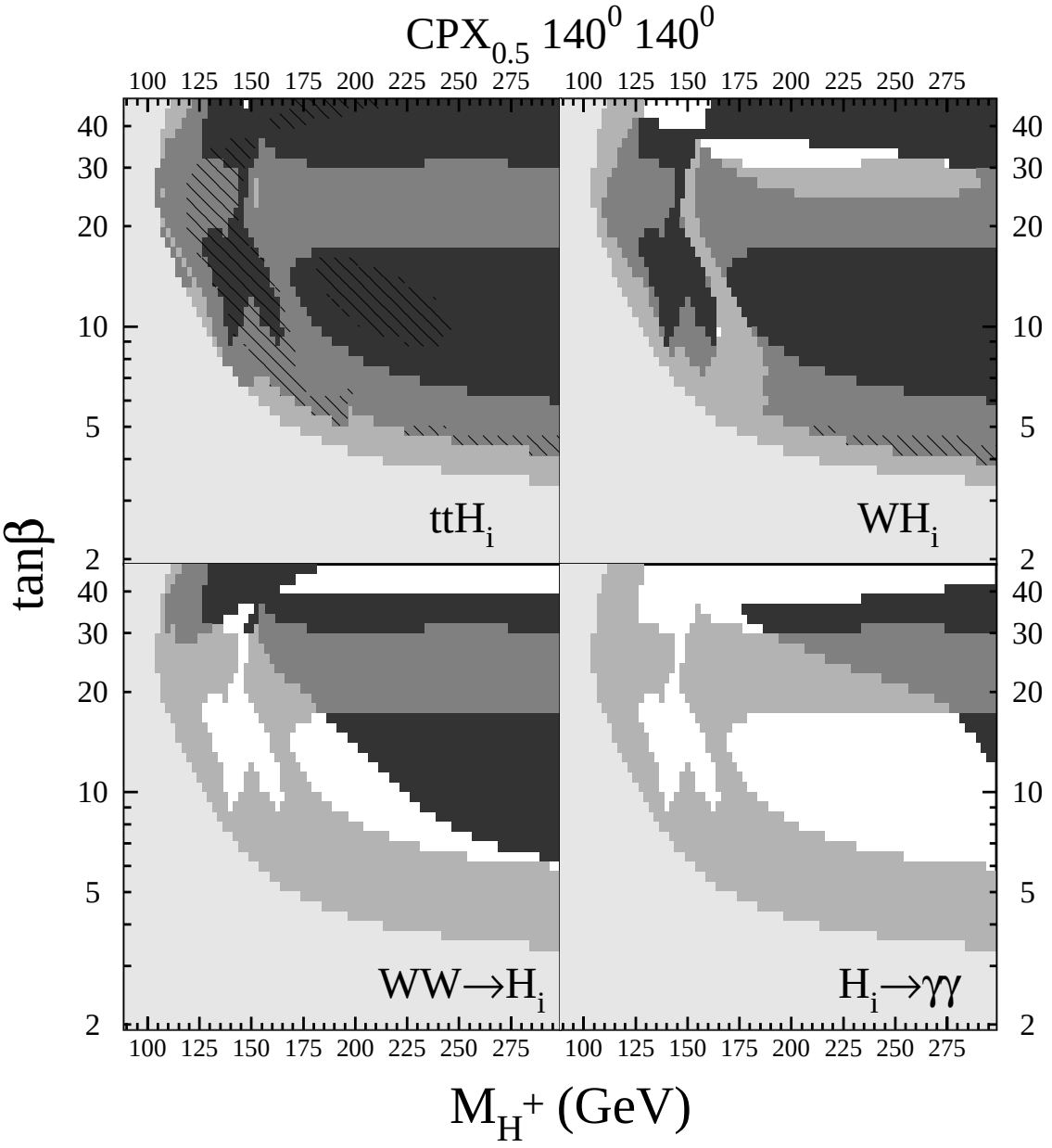

Figure 11: *Same as Fig. 6, but for CP-violating phases (arg($A_{t,b}$), arg($m_{\tilde{g}}$)) = (*$140^\circ, 140^\circ$*).*

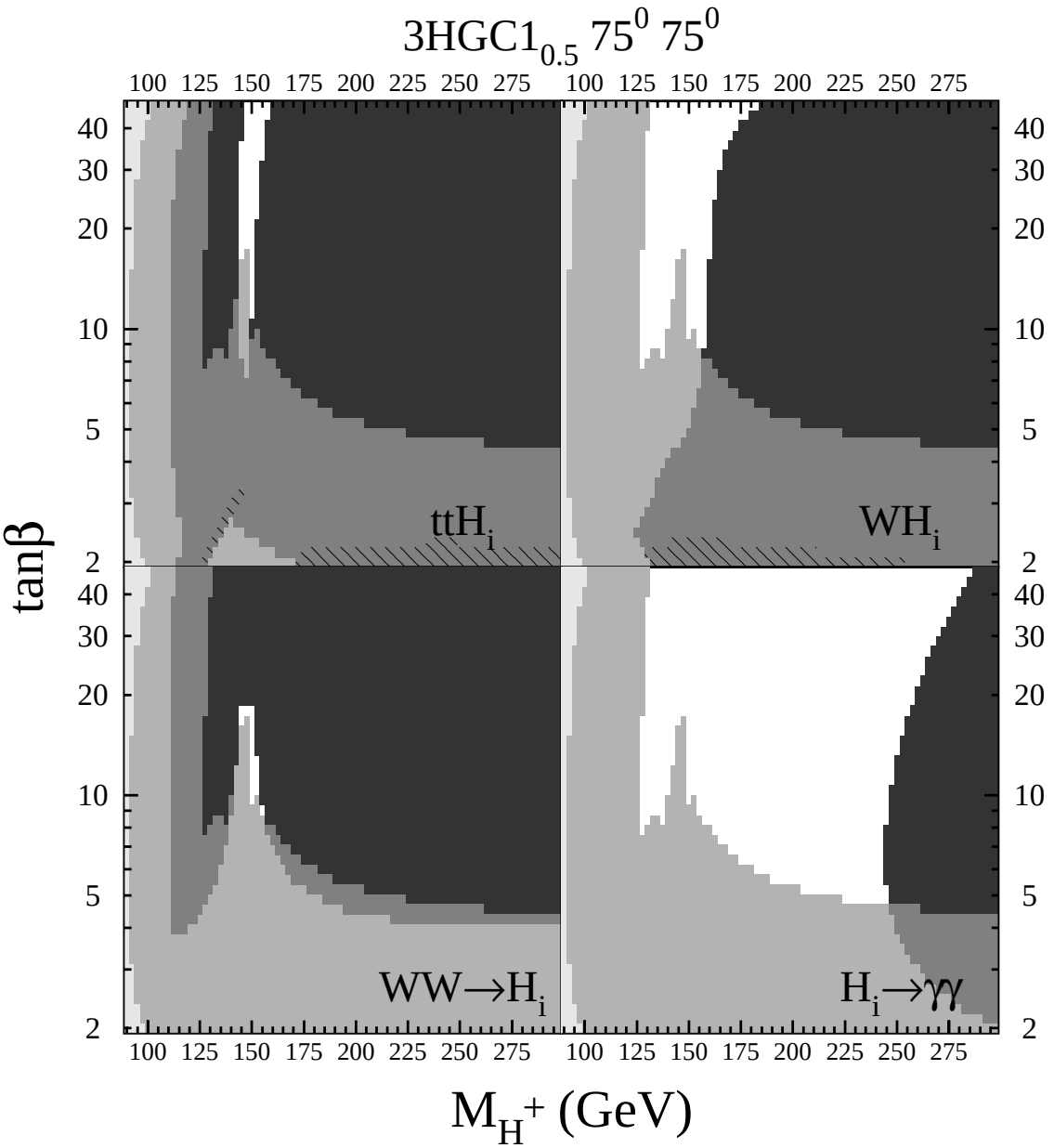

Figure 12: *Same as Fig. 6, but for the 3HGC1 scenario defined in Fig. 3. Here, a region remains uncovered due to dilution of the g_{H_iVV} ($V = W, Z$) coupling among three Higgs bosons.*

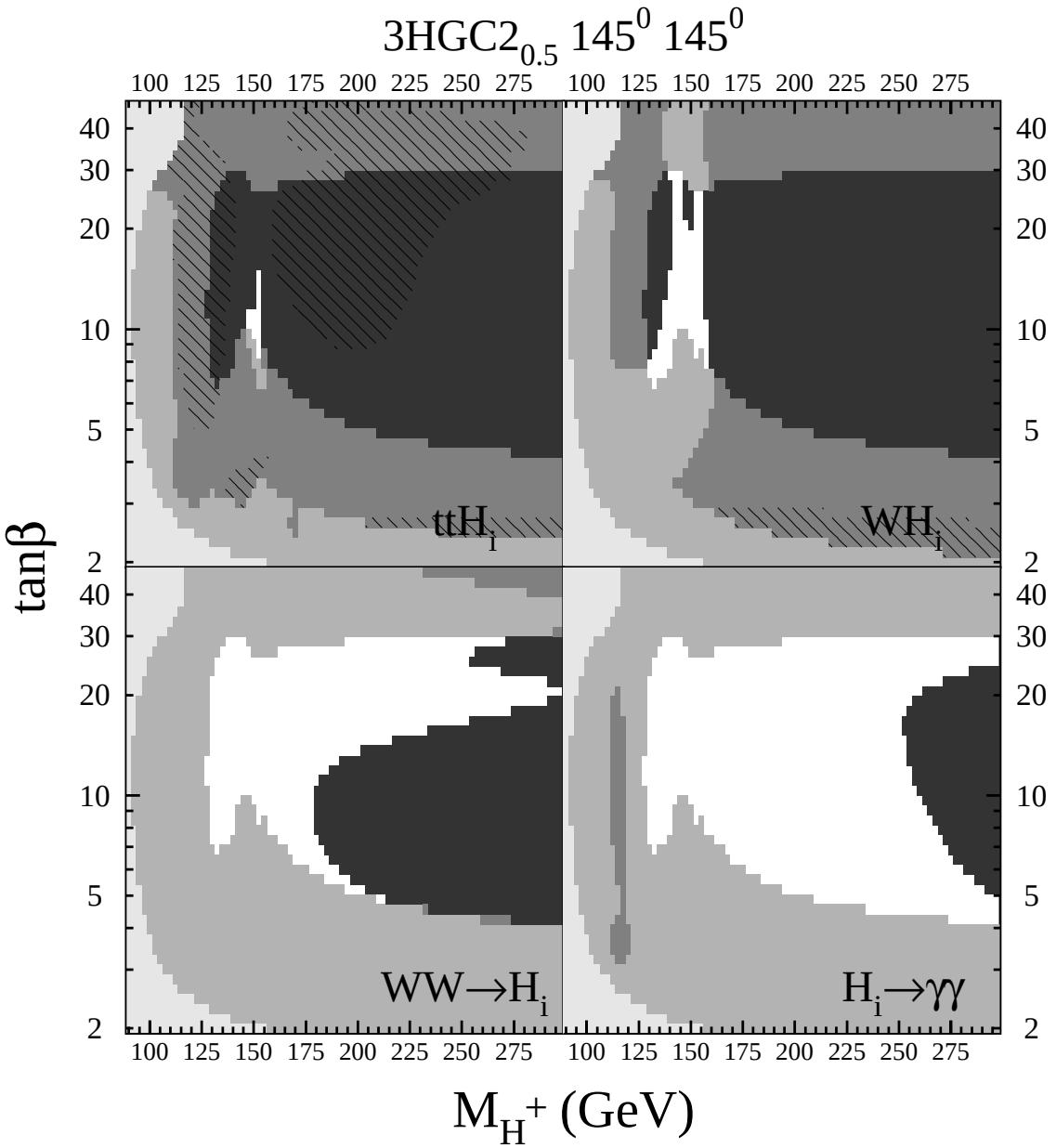

Figure 13: *Same as Fig. 6, but for the 3HGC2 scenario defined in Fig. 3. As in Fig. 12, a region remains uncovered due to dilution of the g_{H_iVV} coupling among three Higgs bosons.*

might still be possible with LEP data if searches for all the possible decay channels of the Higgs bosons were optimized. Our analysis for the Tevatron and the LHC is based on existing experimental simulations of the search for neutral Higgs bosons at these colliders, and could also be extended if more simulations were available.

We have shown that, in general, there is complementarity between the various searches at the two colliders for neutral Higgs bosons with Standard Model–like properties. However, there are still small regions of parameter space, for small values of the charged Higgs boson mass and moderate values of $\tan\beta$, in which none of the three neutral Higgs bosons can be detected with a high statistical significance. In these regions of parameters, one of two phenomena occurs. First, the neutral Higgs boson with dominant couplings to the W and Z bosons can decay predominantly into channels which contain either two neutral Higgs bosons, or a neutral Higgs boson and a Z boson. The lighter Higgs boson has only feeble couplings to the W and Z bosons and top quarks, and escapes detection both at LEP and the hadron colliders. Secondly, all three neutral Higgs bosons can share the coupling to W and Z bosons and the top quark, resulting in three marginal signal excesses. The masses of the Higgs bosons may be uncomfortably close, leading to the possibility that one "signal" is a background to another. Detailed experimental simulations of these situations should be performed in order to decide the detectability of Higgs bosons in these regions of parameters.

Apart from these regions, the Standard Model search channels at the LHC are adequate for discovering a neutral Higgs boson over the range of supersymmetric parameters considered here. The $t\bar{t}H_i(\to b\bar{b})$ and $WW \to H_i(\to \tau^+\tau^-)$ channels are most important. The $gg \to H_i \to \gamma\gamma$ channel is greatly suppressed, and provides no additional coverage. This is a generic feature of the CPX and related scenarios where the b-quark Yukawa coupling can be enhanced over its Standard Model value. However, the Tevatron $W/ZH_i(\to b\bar{b})$ and the LHC $WW \to H_i(\to \tau^+\tau^-)$ channels fall in a special category for two reasons. First, the production of the Higgs boson through a tree–level coupling to the W and Z boson coupling demonstrates that this Higgs boson contributed to the Higgs mechanism. Secondly, radiative corrections can enhance or suppress the b-quark Yukawa coupling, while not affecting the τ-lepton Yukawa coupling, so that $\mathrm{BR}(H_i \to b\bar{b})$ and $\mathrm{BR}(H_i \to \tau^+\tau^-)$ can be complementary to each other. We have presented results for 3-σ evidence with 5 fb^{-1} of luminosity at the Tevatron, and 5-σ discovery with 30 fb^{-1} of luminosity for the $\tau^+\tau^-$ signature at the LHC and with 100 fb^{-1} for the $b\bar{b}$ and $\gamma\gamma$ channels. Our results indicate that the $W/ZH_i(\to b\bar{b})$ and $WW \to H_i(\to \tau^+\tau^-)$ channels alone do not cover the entire range of supersymmetric parameters, even excluding the difficult regions highlighted previously.

The restriction of $WW \to H_i(\to \tau^+\tau^-)$ results to only 30 fb^{-1}, which corresponds to accumulating data for a few years at a moderate instantaneous luminosity, is motivated by the potential deterioration of detection efficiency for this signal at a higher instantaneous luminosity. It is notable that, when comparing the reach with only 30 fb^{-1} of data for all search channels, the $t\bar{t}H_i(\to b\bar{b})$ channel provides very little coverage beyond LEP - though the LHC coverage is for discovery, whereas the LEP coverage is for exclusion - and the $gg \to H_i(\to \gamma\gamma)$ channel provides no discovery potential. It is clear that the vector-boson fusion channel should be studied more thoroughly with detailed detector simulations, including the potential complications raised here regarding several marginal signals in a similar kinematic region.

A Proper Higgs-boson self-couplings

We exhibit here analytic expressions for the proper Higgs-boson self-couplings g^{3H}_{ijk}, $g^{HH^+H^-}_i$, g^{4H}_{ijkl}, $g^{2HH^+H^-}_{ij}$. The Latin indices $i,j,k,l = 1,2,3$ attached to the proper Higgs self-couplings correspond to weak states ϕ_1, ϕ_2 and a.

First, we list the proper trilinear self-couplings $g^{HH^+H^-}_i$ and g^{3H}_{ijk}:

$$\begin{aligned}
g^{HH^+H^-}_1 &= 2s^2_\beta c_\beta \lambda_1 \,+\, c^3_\beta \lambda_3 \,-\, s^2_\beta c_\beta \lambda_4 \,-\, 2s^2_\beta c_\beta \,\mathrm{Re}\lambda_5 \,+\, s_\beta (s^2_\beta - 2c^2_\beta)\,\mathrm{Re}\lambda_6 \,+\, s_\beta c^2_\beta \mathrm{Re}\lambda_7\,, \\
g^{HH^+H^-}_2 &= 2s_\beta c^2_\beta \lambda_2 \,+\, s^3_\beta \lambda_3 \,-\, s_\beta c^2_\beta \lambda_4 \,-\, 2s_\beta c^2_\beta \,\mathrm{Re}\lambda_5 \,+\, s^2_\beta c_\beta \,\mathrm{Re}\lambda_6 \,+\, c_\beta (c^2_\beta - 2s^2_\beta)\,\mathrm{Re}\lambda_7\,, \\
g^{HH^+H^-}_3 &= 2s_\beta c_\beta \,\mathrm{Im}\lambda_5 \,-\, s^2_\beta \,\mathrm{Im}\lambda_6 \,-\, c^2_\beta \,\mathrm{Im}\lambda_7\,, \qquad\qquad (A.1)
\end{aligned}$$

$$\begin{aligned}
g^{3H}_{111} &= c_\beta \lambda_1 \,+\, \frac{1}{2}\, s_\beta \,\mathrm{Re}\lambda_6\,, \\
g^{3H}_{112} &= s_\beta\, \lambda_{34} \,+\, s_\beta \,\mathrm{Re}\lambda_5 \,+\, \frac{3}{2}\, c_\beta \,\mathrm{Re}\lambda_6\,, \\
g^{3H}_{122} &= c_\beta\, \lambda_{34} \,+\, c_\beta \,\mathrm{Re}\lambda_5 \,+\, \frac{3}{2}\, s_\beta \,\mathrm{Re}\lambda_7\,, \\
g^{3H}_{222} &= s_\beta \lambda_2 \,+\, \frac{1}{2}\, c_\beta \,\mathrm{Re}\lambda_7\,, \\
g^{3H}_{113} &= -s_\beta c_\beta \,\mathrm{Im}\lambda_5 \,-\, \frac{1}{2}\,(1 + 2c^2_\beta)\,\mathrm{Im}\lambda_6\,, \\
g^{3H}_{123} &= -2\mathrm{Im}\lambda_5 \,-\, s_\beta c_\beta \,\mathrm{Im}\,(\lambda_6 + \lambda_7)\,, \\
g^{3H}_{223} &= -s_\beta c_\beta \,\mathrm{Im}\lambda_5 \,-\, \frac{1}{2}\,(1 + 2s^2_\beta)\,\mathrm{Im}\lambda_7\,, \\
g^{3H}_{133} &= s^2_\beta c_\beta \lambda_1 \,+\, c^3_\beta\, \lambda_{34} \,-\, c_\beta (1 + s^2_\beta)\,\mathrm{Re}\lambda_5 \,+\, \frac{1}{2}\, s_\beta (s^2_\beta - 2c^2_\beta)\,\mathrm{Re}\lambda_6 \,+\, \frac{1}{2} s_\beta c^2_\beta \,\mathrm{Re}\lambda_7\,, \\
g^{3H}_{233} &= s_\beta c^2_\beta \lambda_2 \,+\, s^3_\beta\, \lambda_{34} \,-\, s_\beta (1 + c^2_\beta)\,\mathrm{Re}\lambda_5 \,+\, \frac{1}{2} s^2_\beta c_\beta \,\mathrm{Re}\lambda_6 \,+\, \frac{1}{2}\, c_\beta (c^2_\beta - 2s^2_\beta)\,\mathrm{Re}\lambda_7\,, \\
g^{3H}_{333} &= s_\beta c_\beta \,\mathrm{Im}\lambda_5 \,-\, \frac{1}{2}\, s^2_\beta \,\mathrm{Im}\lambda_6 \,-\, \frac{1}{2}\, c^2_\beta \,\mathrm{Im}\lambda_7\,, \qquad\qquad (A.2)
\end{aligned}$$

with $\lambda_{34} = \frac{1}{2}\,(\lambda_3 + \lambda_4)$ and $s_\beta\,(c_\beta) = \sin\beta\ (\cos\beta)$. Our analytic expressions in (A.1) and (A.2) agree well with those presented in [27].[3]

In the remainder of the Appendix, we present new analytic results for the proper quadrilinear self-couplings g^{4H}_{ijkl} and $g^{2HH^+H^-}_{ij}$. These are given by

$$\begin{aligned}
g^{4H}_{1111} &= \frac{1}{4}\,\lambda_1\,, \qquad g^{4H}_{1112} = \frac{1}{2}\,\mathrm{Re}\lambda_6\,, \qquad g^{4H}_{1122} = \frac{1}{2}\,\lambda_{34} \,+\, \frac{1}{2}\,\mathrm{Re}\lambda_5\,, \\
g^{4H}_{1222} &= \frac{1}{2}\,\mathrm{Re}\lambda_7\,, \qquad g^{4H}_{2222} = \frac{1}{4}\,\lambda_2\,,
\end{aligned}$$

[3] Recently, another study of Higgs self-couplings appeared [28]. The authors expressed their analytic results in terms of CP-conserving mixing angles and Higgs-boson masses, thus rendering a direct comparison with our expressions very difficult.

$$
\begin{aligned}
g^{4H}_{1113} &= -\frac{1}{2}\, c_\beta\, \mathrm{Im}\lambda_6\,, \qquad g^{4H}_{1123} = -c_\beta\, \mathrm{Im}\lambda_5 - \frac{1}{2}\, s_\beta\, \mathrm{Im}\lambda_6\,,\\
g^{4H}_{1223} &= -s_\beta\, \mathrm{Im}\lambda_5 - \frac{1}{2}\, c_\beta\, \mathrm{Im}\lambda_7\,, \qquad g^{4H}_{2223} = -\frac{1}{2}\, s_\beta\, \mathrm{Im}\lambda_7\,,\\
g^{4H}_{1133} &= \frac{1}{2}\, s^2_\beta\, \lambda_1 + \frac{1}{2}\, c^2_\beta\, \lambda_{34} - \frac{1}{2}\, c^2_\beta\, \mathrm{Re}\lambda_5 - \frac{1}{2}\, s_\beta c_\beta\, \mathrm{Re}\lambda_6\,,\\
g^{4H}_{1233} &= -2 s_\beta c_\beta\, \mathrm{Re}\lambda_5 + \frac{1}{2}\, s^2_\beta\, \mathrm{Re}\lambda_6 + \frac{1}{2}\, c^2_\beta\, \mathrm{Re}\lambda_7\,,\\
g^{4H}_{2233} &= \frac{1}{2}\, c^2_\beta\, \lambda_2 + \frac{1}{2}\, s^2_\beta\, \lambda_{34} - \frac{1}{2}\, s^2_\beta\, \mathrm{Re}\lambda_5 - \frac{1}{2}\, s_\beta c_\beta\, \mathrm{Re}\lambda_7\,,\\
g^{4H}_{1333} &= s_\beta c^2_\beta\, \mathrm{Im}\lambda_5 - \frac{1}{2}\, s^2_\beta c_\beta\, \mathrm{Im}\lambda_6 - \frac{1}{2}\, c^3_\beta\, \mathrm{Im}\lambda_7\,,\\
g^{4H}_{2333} &= s^2_\beta c_\beta\, \mathrm{Im}\lambda_5 - \frac{1}{2}\, s^3_\beta\, \mathrm{Im}\lambda_6 - \frac{1}{2}\, s_\beta c^2_\beta\, \mathrm{Im}\lambda_7\,,\\
g^{4H}_{3333} &= \frac{1}{4}\, \Gamma^{4H^+}\,,
\end{aligned}
\tag{A.3}
$$

where Γ^{4H^+} has been presented in (2.34), and

$$
\begin{aligned}
g^{2HH^+H^-}_{11} &= s^2_\beta\, \lambda_1 + \frac{1}{2}\, c^2_\beta\, \lambda_3 - s_\beta c_\beta\, \mathrm{Re}\lambda_6\,,\\
g^{2HH^+H^-}_{12} &= -\, s_\beta c_\beta\, \lambda_4 - 2 s_\beta c_\beta\, \mathrm{Re}\lambda_5 + s^2_\beta\, \mathrm{Re}\lambda_6 + c^2_\beta\, \mathrm{Re}\lambda_7\,,\\
g^{2HH^+H^-}_{22} &= c^2_\beta\, \lambda_2 + \frac{1}{2}\, s^2_\beta\, \lambda_3 - s_\beta c_\beta\, \mathrm{Re}\lambda_7\,,\\
g^{2HH^+H^-}_{13} &= 2 s_\beta c^2_\beta\, \mathrm{Im}\lambda_5 - s^2_\beta c_\beta\, \mathrm{Im}\lambda_6 - c^3_\beta \mathrm{Im}\lambda_7\,,\\
g^{2HH^+H^-}_{23} &= 2 s^2_\beta c_\beta\, \mathrm{Im}\lambda_5 - s^3_\beta\, \mathrm{Im}\lambda_6 - s_\beta c^2_\beta \mathrm{Im}\lambda_7\,,\\
g^{2HH^+H^-}_{33} &= \Gamma^{4H^+}\,.
\end{aligned}
\tag{A.4}
$$

Notice that the proper self-couplings $g^{HH^+H^-}_i$ and g^{3H}_{ijk} may be also expressed in terms of $g^{2HH^+H^-}_{ij}$ and g^{4H}_{ijkl}, as follows:

$$
\begin{aligned}
g^{HH^+H^-}_1 &= 2c_\beta\, g^{2HH^+H^-}_{11} + s_\beta\, g^{2HH^+H^-}_{12}\,,\\
g^{HH^+H^-}_2 &= 2s_\beta\, g^{2HH^+H^-}_{22} + c_\beta\, g^{2HH^+H^-}_{12}\,,\\
g^{HH^+H^-}_3 &= c_\beta\, g^{2HH^+H^-}_{13} + s_\beta\, g^{2HH^+H^-}_{23}\,,\\
g^{3H}_{111} &= 4c_\beta\, g^{4H}_{1111} + s_\beta\, g^{4H}_{1112}\,,\\
g^{3H}_{112} &= 3c_\beta\, g^{4H}_{1112} + 2s_\beta\, g^{4H}_{1122}\,,\\
g^{3H}_{122} &= 3s_\beta\, g^{4H}_{1222} + 2c_\beta\, g^{4H}_{1122}\,,\\
g^{3H}_{222} &= 4s_\beta\, g^{4H}_{2222} + c_\beta\, g^{4H}_{1222}\,,\\
g^{3H}_{113} &= 3c_\beta\, g^{4H}_{1113} + s_\beta\, g^{4H}_{1123}\,,\\
g^{3H}_{123} &= 2c_\beta\, g^{4H}_{1123} + 2s_\beta\, g^{4H}_{1223}\,,\\
g^{3H}_{223} &= 3s_\beta\, g^{4H}_{2223} + c_\beta\, g^{4H}_{1223}\,,
\end{aligned}
\tag{A.5}
$$

$$
\begin{aligned}
g^{3H}_{133} &= 2c_\beta\, g^{4H}_{1133} + s_\beta\, g^{4H}_{1233}\,, \\
g^{3H}_{233} &= 2s_\beta\, g^{4H}_{2233} + c_\beta\, g^{4H}_{1233}\,, \\
g^{3H}_{333} &= c_\beta\, g^{4H}_{1333} + s_\beta\, g^{4H}_{2333}\,.
\end{aligned}
\tag{A.6}
$$

The above relations are useful for checking the self-consistency of all the analytic expressions pertinent to the trilinear and quadrilinear Higgs self-couplings.

B Experimental Simulations used in our Analysis

We summarize here the results from previous simulations of Higgs production at the LHC, upon which we have based our analysis of MSSM neutral-Higgs production in the presence of CP violation. In each Table, we provide the minimum ratio R, relative to the Standard Model product of cross section times branching ratio, for which a signal of the stated significance could be obtained with the quoted luminosity. We have provided more information regarding the expected number of signal S and background B events for those cases when S/B$\sim$ 1.

M_H (GeV)	90	100	110	120	130
$R_{3\sigma}$(5 fb^{-1})	0.63	0.71	0.88	1.07	1.43

Table 1: *R values for 3-σ evidence for a Higgs boson in the channel $W/ZH(\to b\bar{b})$ at the Tevatron with 5 fb^{-1} of accumulated data [22]. These results are based on combining the CDF and DØ data.*

M_H (GeV)	S (100 fb^{-1})	B (100 fb^{-1})	$\sigma_{\rm Gauss}$	$R_{5\sigma}$ (100 fb^{-1})
100	147	223	9.84	0.51
105	123	191	8.92	0.56
110	100	160	7.91	0.63
115	98	163	7.68	0.65
120	96	167	7.43	0.67
125	86	157	6.89	0.73
130	77	148	6.33	0.79

Table 2: *The expected signal, background, Gaussian significance and the R value for 5-σ discovery of a Higgs boson in the channel $t\bar{t}H(\to b\bar{b})$ at the LHC with 100 fb^{-1} of accumulated data [23]. These results are for the CMS experiment only. The Gaussian significance is based on a K factor of unity for the signal [35].*

M_H (GeV)	S (30 fb^{-1})	B (30 fb^{-1})	$\sigma_{\rm Gauss}$	$R_{5\sigma}$
110	11.1	3.9	4.1	1.22
120	10.4	1.4	5.2	0.96
130	8.6	0.9	5.0	1.00
140	5.8	0.7	3.9	1.28
150	3.0	0.6	2.3	2.17

Table 3: *The expected signal, background, Gaussian significance and the R value for 5-σ discovery of a Higgs boson in the channel $WW \to H(\to \tau^+\tau^-)$ at the LHC with 30 fb^{-1} of accumulated data [24]. A detector–level analysis based on a fast simulation was presented in [36]. The results there for the combination of one hadronic and one leptonic decay of the $\tau^+\tau^-$ pair are slightly less significant than the original analysis, but they have not been combined with the all leptonic decays. Therefore, we have chosen to use the original numbers, even though they are based on a parton–level analysis.*

M_H (GeV)	80	90	100	110	120	130	150
$R_{5\sigma}$ (100 fb^{-1})	1.02	0.74	0.60	0.49	0.42	0.4	0.66

Table 4: *The expected signal, background, Gaussian significance and the R value for 5-σ discovery of a Higgs boson in the channel $gg \to H(\to \gamma\gamma)$ at the LHC with 100 fb^{-1} of accumulated data [26]. These apply to CMS only.*

References

[1] H.P. Nilles, Phys. Rept. **110** (1984) 1; H.E. Haber and G.L. Kane, Phys. Rept. **117** (1985) 75. For a recent review, see M. Carena and H.E. Haber, hep-ph/0208209.

[2] A. Pilaftsis, Phys. Rev. **D58** (1998) 096010; Phys. Lett. **B435** (1998) 88.

[3] A. Pilaftsis and C.E.M. Wagner, Nucl. Phys. **B553** (1999) 3.

[4] D.A. Demir, Phys. Rev. **D60** (1999) 055006.

[5] S.Y. Choi, M. Drees and J.S. Lee, Phys. Lett. **B481** (2000) 57; G.L. Kane and L.-T. Wang, Phys. Lett. **B488** (2000) 383; S. Heinemeyer, Eur. Phys. J. **C22** (2001) 521; M. Boz, Mod. Phys. Lett. **A17** (2002) 215; S.W. Ham, S.K. Oh, E.J. Yoo, C.M. Kim and D. Son, hep-ph/0205244.

[6] M. Carena, J. Ellis, A. Pilaftsis and C.E.M. Wagner, Nucl. Phys. **B586** (2000) 92.

[7] T. Ibrahim and P. Nath, Phys. Rev. **D63** (2001) 035009; T. Ibrahim, Phys. Rev. **D64** (2001) 035009; T. Ibrahim and P. Nath, Phys. Rev. D **D66** (2002) 015005.

[8] M. Carena, J. Ellis, A. Pilaftsis and C.E.M. Wagner, Phys. Lett. **B495** (2000) 155.

[9] M. Carena, J. Ellis, A. Pilaftsis and C.E.M. Wagner, Nucl. Phys. **B625** (2002) 345.

[10] A. Dedes and S. Moretti, Phys. Rev. Lett. **84** (2000) 22; Nucl. Phys. **B576** (2000) 29; S.Y. Choi and J.S. Lee, Phys. Rev. **D61** (2000) 115002; S.Y. Choi, K. Hagiwara and J.S. Lee, Phys. Lett. **B529** (2002) 212; A. Arhrib, D. K. Ghosh and O.C. Kong, Phys. Lett. **B537** (2002) 217.

[11] B. Grzadkowski, J. F. Gunion and J. Kalinowski, Phys. Rev. **D60** (1999) 075011; A.G. Akeroyd and A. Arhrib, Phys. Rev. **D64** (2001) 095018; S. Y. Choi, B. c. Chung, P. Ko and J. S. Lee, Phys. Rev. D **66** (2002) 016009.

[12] D. Atwood and A. Soni, Phys. Rev. **D52** (1995) 6271; B. Grzadkowski and J.F. Gunion, Phys. Lett. **B350** (1995) 218; A. Pilaftsis, Phys. Rev. Lett. **77** (1996) 4996; Nucl. Phys. **B504** (1997) 61; E. Asakawa, S.Y. Choi and J.S. Lee, Phys. Rev. **D63** (2001) 015012; M.S. Berger, Phys. Rev. Lett. **87** (2001) 131801; C. Blochinger *et al.*, hep-ph/0202199.

[13] S.Y. Choi, K. Hagiwara and J.S. Lee, Phys. Rev. **D64** (2001) 032004; S. Y. Choi, M. Drees, J. S. Lee and J. Song, Eur. Phys. J. C **25** (2002) 307; E. Christova, H. Eberl, W. Majerotto and S. Kraml, Nucl. Phys. **B639** (2002) 263; hep-ph/0211063.

[14] For recent analyses of one- and two-loop EDM effects, see T. Ibrahim and P. Nath, Phys. Rev. **D58** (1998) 111301; Phys. Rev. **D61** (2000) 093004; M. Brhlik, G.J. Good and G.L. Kane, Phys. Rev. **D59** (1999) 115004; S. Pokorski, J. Rosiek and C.A. Savoy, Nucl. Phys. **B570** (2000) 81; E. Accomando, R. Arnowitt and B. Dutta, Phys. Rev. **D61** (2000) 115003; A. Bartl, T. Gajdosik, W. Porod, P. Stockinger and H. Stremnitzer, Phys. Rev. **D60** (1999) 073003; D. Chang, W.-Y. Keung and A. Pilaftsis, Phys. Rev. Lett. **82** (1999) 900; S.A. Abel, S. Khalil and O. Lebedev, Nucl. Phys. **B606** (2001) 151; D.A. Demir, M. Pospelov and A. Ritz, hep-ph/0208257.

[15] For a recent analysis of Higgs-mediated EDMs in the CP-violating MSSM, see A. Pilaftsis, Nucl. Phys. **B644** (2002) 263.

[16] T. Falk, K.A. Olive, M. Pospelov and R. Roiban, Nucl. Phys. **B60** (1999) 3.

[17] For example, see, A.J. Buras, P.H. Chankowski, J. Rosiek and L. Slawianowska, Nucl. Phys. **B619** (2001) 434; hep-ph/0210145; P.H. Chankowski and L. Slawianowska, Acta Phys. Polon. **B32** (2001) 1895; C.S. Huang and W. Liao, Phys. Lett. **B538** (2002) 301; D.A. Demir and K.A. Olive, Phys. Rev. **D65** (2002) 034007; T. Ibrahim and P. Nath, hep-ph/0208142.

[18] A. Dedes and A. Pilaftsis, hep-ph/0209306.

[19] Information about the code `CPHDECAY` can be obtained from S. Mrenna at `mrenna@fnal.gov`.

[20] A. Djouadi, J. Kalinowski and M. Spira, Comput. Phys. Commun. **108** (1998) 56.

[21] The Fortran code `cph.f` is available at `http://home.cern.ch/p/pilaftsi/www/`.

[22] M. Carena *et al.*, hep-ph/0010338.

[23] V. Drollinger, T. Muller and D. Denegri, hep-ph/0111312.

[24] D. Rainwater and D. Zeppenfeld, Phys. Rev. **D60** (1999) 113004 and **D61** (2000) 099901 (E); T. Plehn, D. Rainwater and D. Zeppenfeld, Phys. Lett. **B454** (1999) 297 and Phys. Rev. **D61** (2000) 093005.

[25] M. Carena, S. Mrenna and C.E.M. Wagner, Phys. Rev. **D60** (1999) 075010 and Phys. Rev. **D62** (2000) 055008.

[26] K. Lassila-Perini, CMS Thesis-1998-147.

[27] S.Y. Choi and J.-S. Lee, Phys. Rev. **D61** (2000) 015003.

[28] M.N. Dubinin and A.V. Semenov, hep-ph/0206205.

[29] OPAL Collaboration, OPAL Physics Note PN505 (2002).

[30] ALEPH, DELPHI, L3 and OPAL Collaborations, the LEP working group for Higgs boson searches, LHWG Note 2002-01 (2002), and additional updates at `http://lephiggs.web.cern.ch/LEPHIGGS/www/Welcome.html`.

[31] ALEPH, DELPHI, L3 and OPAL Collaborations, the LEP working group for Higgs boson searches, LHWG Note 2001-04 (2001).

[32] OPAL Collaboration, CERN-EP/2000-092 (2000).

[33] J. Dai, J. F. Gunion and R. Vega, Phys. Lett. B **371**, 71 (1996); **387**, 801 (1996); E. Richter-Wąs and D. Froidevaux, Z. Phys. C **76**, 665 (1997); A. Belyaev, M. Drees, and J. K. Mizukoshi, Eur. Phys. J. C **17**, 337 (2000); R. Lafaye, D.J. Miller, M. Muhlleitner and S. Moretti, A. A. Barrientos Bendezu and B. A. Kniehl, Phys. Rev. D **64**, 035006 (2001).

[34] ATLAS Collaboration, A. Airapetian *et al.*, ATLAS Detector and Physics Performance: Technical Design Report, Vol. II, Report No. CERN/LHCC/99-15.

[35] W. Beenakker, S. Dittmaier, M. Kramer, B. Plumper, M. Spira and P. M. Zerwas, Phys. Rev. Lett. **87** (2001) 201805; L. Reina and S. Dawson, Phys. Rev. Lett. **87** (2001) 201804; L. Reina, S. Dawson and D. Wackeroth, Phys. Rev. D **65** (2002) 053017.

[36] D. Cavalli *et al.*, hep-ph/0203056.